Available online at www.sciencedirect.com
ScienceDirect
Micron 39 (2008) 209–228
micron
www.elsevier.com/locate/micron

Review

Structure and composition of calcareous sponge spicules: A review and comparison to structurally related biominerals

Ingo Sethmann [a,*], Gert Wörheide [b]

[a] *Institut für Mineralogie, Universität Münster, Corrensstr. 24, D-48149 Münster, Germany*
[b] *Geowissenschaftliches Zentrum Göttingen, Abteilung Geobiologie, Universität Göttingen, Goldschmidtstr. 3, D-37077 Göttingen, Germany*

Received 9 November 2006; received in revised form 18 January 2007; accepted 18 January 2007

Abstract

Since the early 19th century, the skeletons of calcareous sponges (Porifera: Calcarea) with their mineralized spicules have been investigated for their morphologies, structures, and mineralogical and organic compositions. These biomineral spicules, up to about 10 mm in size, with one to four rays called actines, have various specific shapes and consist mainly of magnesium-calcite: in only one case has an additional phase of stabilized amorphous $CaCO_3$ (ACC) been discovered. The spicules are invariably covered by a thin organic sheath and display a number of intriguing properties. Despite their complex morphologies and rounded surfaces without flat crystal faces they behave largely as single crystal individuals of calcite, and to some degree crystallographic orientation is related to morphology. Despite their single-crystalline nature, most spicules show nearly isotropic fracture behaviour, not typical for calcite crystals, indicating enhanced fracture resistance. These unusual morphological and mechanical properties are the result of their mechanism of growth. Each spicule is formed by specialized cells (sclerocytes) that supply mineral ions or particles associated by organic macromolecules to extracellular cavities, where assembly and crystallization in alignment with an initial seed crystal (nucleus) takes place. As a result of discontinuous mineral deposition, cross-sections of larger spicules display concentric layering that mantles a central calcitic rod. On a smaller scale, the entire spicule displays a 'nano-cluster' structure with crystallographically aligned and putatively semicoherent crystal domains as well as a dispersed organic matrix intercalated between domain boundaries. This ultrastructure dissipates mechanical stress and deflects propagating fractures. Additionally, this nano-cluster construction, probably induced by intercalated organic substances, enables the formation of complex crystal morphologies independent of crystal faces. In this review, the current knowledge about the structure, composition, and formation of calcareous sponge spicules is summarised and discussed. Comparisons of calcareous sponge spicules with the amorphous silica spicules of sponges of the classes Hexactinellida and Demospongiae, as well as with calcitic skeletal elements of echinoderms are drawn. Despite the variety of poriferan spicule mineralogy and the distant phylogenetic relationship between sponges and echinoderms, all of these biominerals share similarities regarding their nano-scale construction. Furthermore, echinoderm skeletal elements resemble calcareous sponge spicules in that they represent magnesium-bearing calcite single-crystals with extremely complex morphologies.

Keywords: Biomineralization; Calcarea; Calcite; Echinodermata; Porifera; Single-crystals; Silica; Skeletons; Sponges; Ultrastructure

Contents

* Corresponding author. Fax: +49 251 1449635.
E-mail address: isethma@uni-muenster.de (I. Sethmann).

0968-4328/$ – see front matter © 2007 Elsevier Ltd. All rights reserved.
doi:10.1016/j.micron.2007.01.006

1. Introduction

Sponges (Porifera Grant, 1836) possess the most primitive morphology of all animals (Metazoa), lacking distinct tissues and organs as they occur in all more complex animals that possess those traits (Eumetazoa) (Hooper and Van Soest, 2002). Adult sponges are sessile, predominantly marine, and feed on suspended organic particles and micro-organisms by actively filtering ambient water through an aquiferous system. In the simplest case, the so-called asconid body plan, the sponge body is tube- or bottle-shaped with an apical opening (osculum), and numerous small pores (ostia) and unbranched canals that perforate the body wall (Fig. 1). Flagellated cells (choanocytes) line the canals and the inner body wall (choanoderm) and produce a water current that flows from the exterior through the ostia and canals into the inner cavity (atrium), and leaves the sponge body through the osculum. In the so-called syconid and leuconid grade of aquiferous system-construction, the choanoderm is folded to increase its surface, resulting in a more complex system of branched canals and distinct choanocyte chambers. A general description of sponge anatomy is given by Boury-Esnault and Rützler (1997). In order to maintain morphological rigidity of the body wall and aquiferous system, most sponges produce mineralized spicular skeletons (see Fig. 1) that consist either of silica (skeletal opal, in the Hexactinellida and Demospongiae) (reviews: Simpson, 1984; Uriz et al., 2003a,b; Müller et al., 2006; Uriz, 2006) or of calcium carbonate (almost exclusively calcite, in the Calcarea) (reviews: Jones, 1970; Simpson, 1984; see also Uriz, 2006). However, some demosponges, for example the 'Keratosa' (a polyphyletic group, not defined by common ancestry), only produce collagenous spongin-fibres and completely lack mineralized spicules (e.g., Hooper and Van Soest, 2002). Another polyphyletic group of sponges formerly known as 'Sclerospongiae' produce a secondary calcareous skeleton of aragonite or Mg-calcite, in addition to their primary spicular skeleton (e.g., Reitner, 1992; Wörheide, 1998).

In the present review, we will focus on the calcareous primary spicules of the poriferan class Calcarea, comprising exclusively marine species. These spicules occur in various elaborate shapes and in a size range of several micrometres to centimetres. Apparently species-specific varieties of spicules, together with their spatial arrangement and mineralogy have been used as distinctive criteria for sponge taxonomy and systematics (e.g., Haeckel, 1872; Wörheide and Hooper, 1999, 2003; Manuel et al., 2002; Borojevic et al., 2002a,b,c; Vacelet et al., 2002a,b) although recent molecular-systematic studies have demonstrated that the existing systematic system of the Calcarea is probably highly artificial (Dohrmann et al., 2006). However, despite their low complexity of body organization and lack of specialized intercellular communication (nerve) system, the high degree of architectural complexity and diversity of forms and shapes of skeletal elements in different sponge groups makes it clear that controlled biomineralization *sensu* Mann (1983) occurs by the concerted action of specialized cells.

Early investigators of sponge biology and taxonomy have already described spicules and skeletal structures using light microscopic techniques. They have also addressed the process of formation of the elaborate spicules, their ultrastructure, and the composition of the spicule materials. These detailed analyses are the basis for refined contemporary studies on $CaCO_3$ biomineralization in sponges. Therefore, the following review comprises the recent developments in sponge spicule research, and also gives an account of early fundamental works (for reviews, see Haeckel (1872) and Minchin (1909)) as a basis for discussion.

2. Spicule types

The spicular skeletons of the Calcarea consist of calcareous spicules with a considerable morphological diversity, in the two subclasses Calcinea and Calcaronea with four basic spicule types, classified by their numbers of actines that grow outwards from a common point of origin. Monactines are spicules with a simple, needle-like, in some cases slightly curved geometry, with the tip growing out from one end (Fig. 2c). There are various different characteristic forms of monactine 'heads'. Diactines have a similar appearance but with two opposite tips (Fig. 2b). In triactines the three actines may be oriented in various ways, the simplest being the regular star-shaped spicules, with the equiradiate actines oriented in one plane, enclosing angles of 120°, respectively (Fig. 2a). Additionally, there are several variations of this basic regular triactine geometry, usually with one straight basal actine, and the other two actines deformed as a morphologically inverse pair, as in 'tuning fork' triactines with two actines curved upwards, or in 'sagittal' triactines with two actines curved downwards, with two equal angles and one unequal angle between them. In other triactines the rays are not oriented in a plane but may show

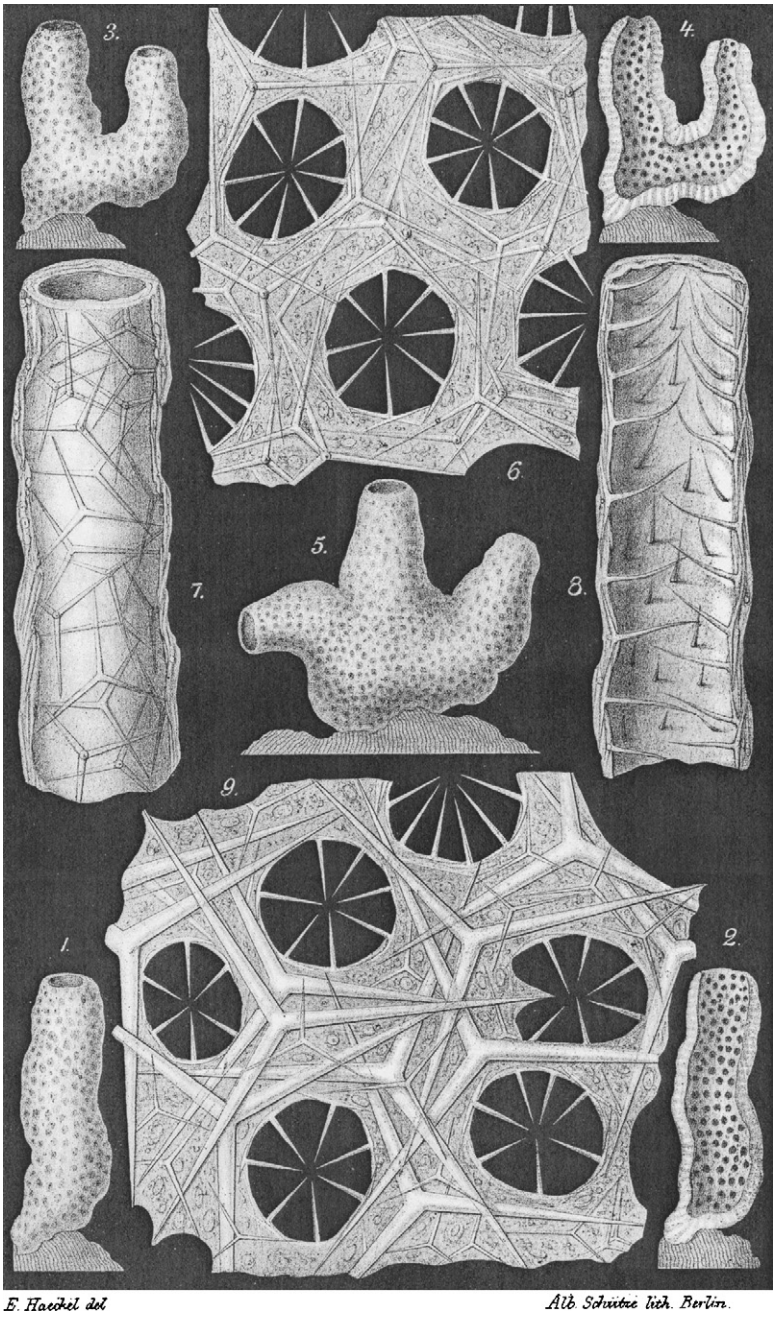

Fig. 1. Morphology and skeletal structure of sponges (example: *Sycaltis* [= *Amphoriscus*] *perforatus* Haeckel, 1872). (1) Complete sponge individual with a single osculum (*Sycurus* [= *Amphoriscus*] *perforatus*). (2) The same individual in longitudinal section. (3) Complete sponge individual with two osculae (*Sycothamnus* [= *Amphoriscus*] *perforatus*). (4) The same individual in longitudinal section. (5) Complete individual with three osculae (*Sycothamnus* [= *Amphoriscus*] *perforatus*). (6) Structure of the choanosome with spicules reinforcing the ostia. (7) Single radial tube viewed from the outside. (8) Single tube, reinforced by spicules, in longitudinal section. (9) Structure of the pinacoderm with spicules reinforcing the ostia. Magnifications: (1–5) ×3, (6–9) ×100. Figure reproduced from Haeckel (1872).

various different geometries of lower symmetry (Fig. 2d). Tetractine spicules are similar to triactines with an additional, usually shorter apical ray protruding from the central origin of the three basic rays. Tetractines also can develop into various shapes (for details see Boury-Esnault and Rützler, 1997). A recent article by Rossi et al. (2006) reports on the previously unnoticed occurrence of pentactines in the newly described species *Sycon pentactinalis*: these pentactines are either based on triactines with additional two apical actines sometimes originating side-by-side from the spicule centre, similar to tetractines, or their morphology is irregular with almost randomly oriented actines.

In addition to these spicule types in Calcinea and Calcaronea, species of the fossil Heteractinida (occurrence in the Palaeozoic from Lower Cambrian to Permian) developed spicules on the basis of hexagonal symmetry: rosette-shaped spicules with six coplanar actines (hexaradiates) as the basic form and octactines with additional two actines perpendicular

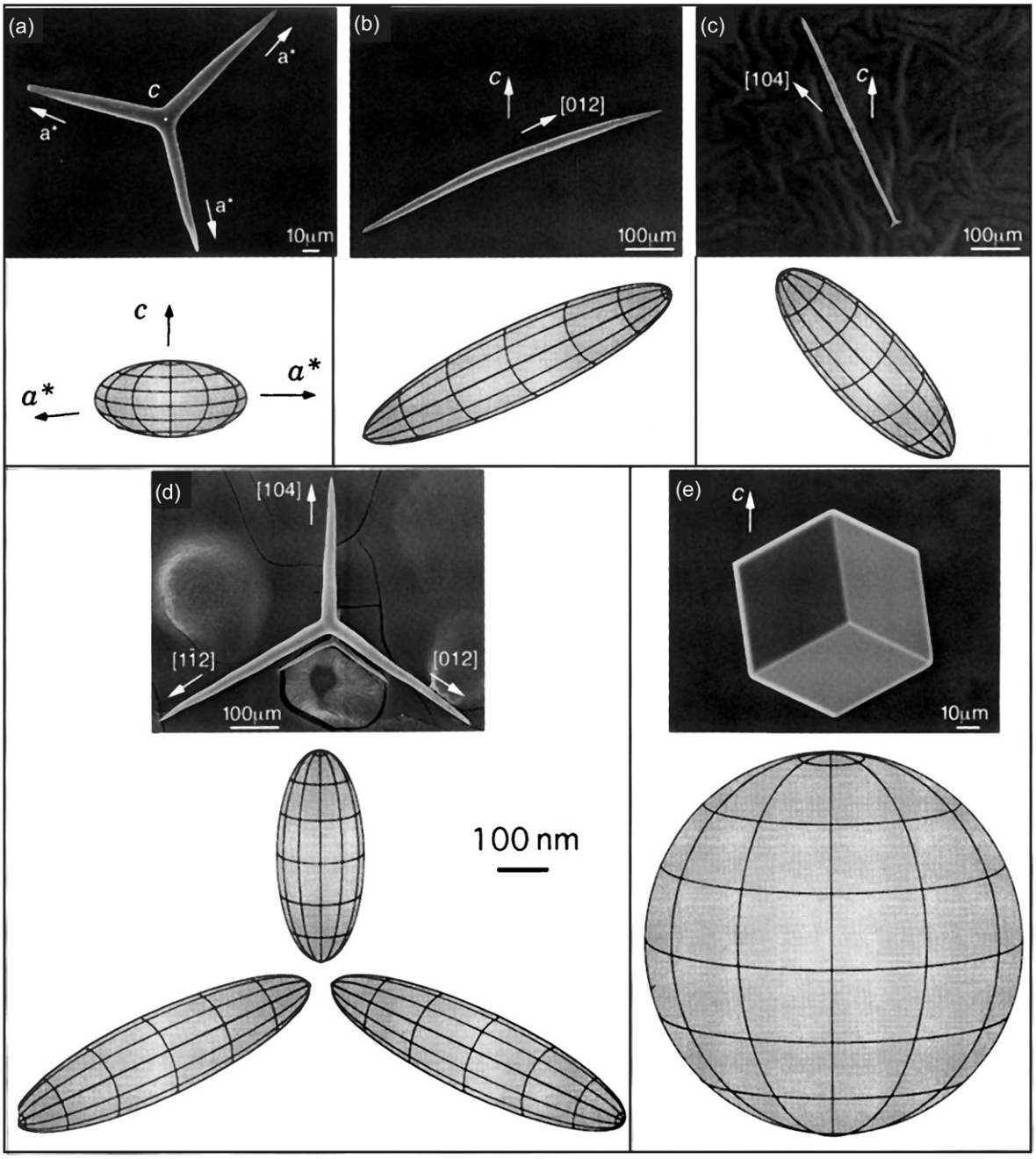

Fig. 2. Scanning electron micrographs of calcitic sponge spicules and a pure calcite crystal, and the reconstructed three-dimensional shapes of each of their average perfect domains derived from XRD-measured coherence lengths in different directions. Crystallographic axes and directions are indicated; crystal domains are all down to the same scale. Note that domain shapes of the biogenic crystals correspond to macroscopic morphologies: (a) regular triactine spicule from a *Clathrina* species. The domain is flattened in the *c* direction. (b) Curved diactine spicule from a *Sycon* species. (c) Nail-like monactine spicule from a *Kebira* species. (d) Asymmetric triactine spicule from a *Sycon* species. (e) Synthetic calcite crystal grown in the absence of additives. Only the stable $\{1\,0\,\bar{1}\,4\}$ faces are expressed; the average crystal domain is isotropic in shape. Figure: Copyright 1996, from Aizenberg et al. (1996b). Reproduced by permission of Taylor & Francis Group, LLC, http://www.taylorandfrancis.com.

to both sides of the rosette plane originating from the spicule centre (see Pickett (2002), and Finks and Rigby (2004) for reviews). In derived forms some actines may be suppressed or additional ones may occur to form polyactines (same authors). Although the authors agree that the original material of the fossilised spicules of the Heteractinida was most probably calcite, Finks and Rigby (2004) preferred to consider heteractinid sponges as a separate class Heteractinida in the phylum Porifera, instead of ranking them as an order Heteractinida within the class Calcarea, as done by Pickett (2002). Due to morphological similarities of the heteractinid spicules with calcarean as well as with siliceous hexactinellid spicules, Botting and Butterfield (2005) discuss the Heteractinida as a problematic, mostly calcarean group that possibly includes a stem group which branched into the Calcarea and the Hexactinellida. However, their hypothesis that traces of a

layered structure found in fossil spicules of the Middle Cambrian heteractinid *Eiffelia globosa* Walcott, 1920, possibly derive from an original spicule structure with a central rod of calcium carbonate and a secondary outer layer of opaline silica (original minerals not preserved), separated by an organic layer, has to be rejected: in Calcarea spicules are secreted extracellularily and in Silicea (Demospongiae + Hexactinellida) initially intracellularily (Simpson, 1984; see Sections 5.1 and 7.1)—two completely different and non-homologous processes (Manuel et al., 2003).

All types of calcareous spicules may occur in a size range of about 0.1–10 mm, depending on the species, and different spicules may be arranged in specific architectures to construct the skeleton (Manuel et al., 2002; Borojevic et al., 2002a,b,c; Vacelet et al., 2002a,b; Pickett, 2002; Finks and Rigby, 2004; Rossi et al., 2006). Therefore, the composition of spicular elements and their architecture in skeletons have been used as the main criteria in calcarean systematics and taxonomy since Haeckel (1869, 1872) proposed the first systematic system of Calcarea.

3. Inorganic components of calcarean spicules

3.1. Inorganic chemistry and crystallography

The recognition of the calcareous sponges as a distinct monophyletic taxon (a systematic group of organisms defined by common ancestry), the Calcarea (or Calcispongia), has been based on the distinct mineralogy of their spicules. Grant (1826a) was the first to recognize that, beside groups of sponges with ''horny fibres'' or ''siliceous spicula'', there are sponges with ''calcareous spicula'', the substance of which he further characterized as ''carbonate of lime'' (Grant, 1826b). Haeckel (1872) discovered that the calcium carbonate substance of these spicules is double-refracting in polarized light and hence crystalline. Taking further into account the morphology of regular triactines, reminiscent of symmetry according to the hexagonal crystal system, he assumed the crystalline phase to be calcite. In a physical study, measuring the optical properties and specific gravity, Sollas (1885a) confirmed the calcitic nature of the spicules, and he pointed out that each of the different spicules behaved optically as a single crystal individual. An extensive study by von Ebner (1887) on spicules of a variety of species corroborated Sollas' crystallographic results by his observation of forms and orientations of etch figures and calcite overgrowths on spicules that were always indicative of a single crystallographic orientation in each whole spicule. von Ebner provides illustrations of a number of spicules that suggest a correlation between spicule morphologies and specific crystallographic directions. Such relations between spicule morphologies and crystallographic orientations were pointed out by Schmidt (1924) in an optical microscopy-based investigation. Optical, etch, and overgrowth methods have been repeatedly applied to different calcareous sponge spicules in other studies (Sollas, 1885b; Bidder, 1898; Jones, 1955a,b; Aizenberg et al., 1994, 1995b, 1996a,b; Sethmann et al., 2006) (Fig. 3d–f), accompanied by single-crystal X-ray diffraction methods (Aizenberg et al., 1995a,b; Sethmann et al., 2006) (Fig. 3b) and electron diffraction (Sethmann et al., 2006) (Fig. 4), which all together resulted in the acceptance of the calcitic nature and largely single-crystalline behaviour of the spicules of Calcarea (Figs. 2 and 3a and c).

However, von Ebner (1887) already took into consideration that each spicule may in fact be a polycrystalline structure with tiny calcite crystallites being crystallographically aligned to a high degree. This idea becomes exceptionally attractive, if one accepts the presence of a dispersed organic matrix inside the 'single-crystals' (which von Ebner did not) (see Section 4.1). The crystal cluster-theory got late support from a transmission electron microscopy (TEM) study by Travis (1970), in which ultramicrotomed spicules were presented as arrays of subunits, mechanically disintegrated but still oriented, with a remarkably narrow size range on a nanometre-scale. Also from synchrotron X-ray diffraction analyses of spicules from species of *Sycon* Risso, 1826, *Kebira* Row, 1909, and *Clathrina* Gray, 1867, done by Aizenberg et al. (1995a,b), crystal coherence lengths in the sub-micrometre range inside the calcite biocrystals were derived. Recently, direct proof of the existence of a nanometre-scaled cluster-like ultrastructure of calcitic sponge spicules came from atomic force microscopy (AFM) and TEM, performed by Sethmann et al. (2006) on triactines of the calcinean *Pericharax heteroraphis* Poléjaeff, 1883: On naturally grown, etched, and fractured surfaces, AFM images showed granular patterns with grain sizes in the range of about 10–100 nm (Figs. 3d and 5a, b and e), which high-resolution TEM revealed to consist of even smaller crystal domains of only few nanometres in size (Fig. 5f). The same TEM study reveals a structural heterogeneity of the spicule material with locally accumulated, but on the whole minor misalignments of crystal domains (Fig. 4). The precise crystallographic alignment of the majority of the crystal domains (defect-free coherent areas in crystals) suggests coherence of the domains by crystal lattice 'bridges' (semicoherence). Such crystal lattice coherence would justify the consideration of the clustered bulk material of a spicule as a real single-crystal.

Sponge spicule calcite contains inorganic impurities: von Ebner (1887) analysed magnesium, sodium, 'sulphuric acid', and probably water in spicules of *Leucandra aspera* Schmidt, 1862. Jones and James (1969) detected magnesium, strontium, and sulphur in large triactines of *Leuconia nivea* Grant, 1826, with an electron microprobe. Jones and Jenkins (1970) presented chemical analyses, X-ray diffraction and infrared spectroscopic data for spicules from a number of different sponge species that qualitatively resulted in Mg^{2+} as a major, Sr^{2+}, Na^{+}, and SO_4^{2-} as minor, and Al^{3+}, Si, Mn^{2+}, Ba^{2+}, and Li^{+} as trace impurities.

Dissolution experiments with different acids also showed that complete dissolution of sponge spicules takes place more rapidly than dissolution of pure calcite crystals in the same solvent (e.g., von Ebner, 1887; Jones, 1955b). On one hand, this enhanced over-all solubility may have kinetic reasons, since the above mentioned cluster structure enlarges the reactive surface area of the spicules (cf., Morse and Arvidson, 2002). On the

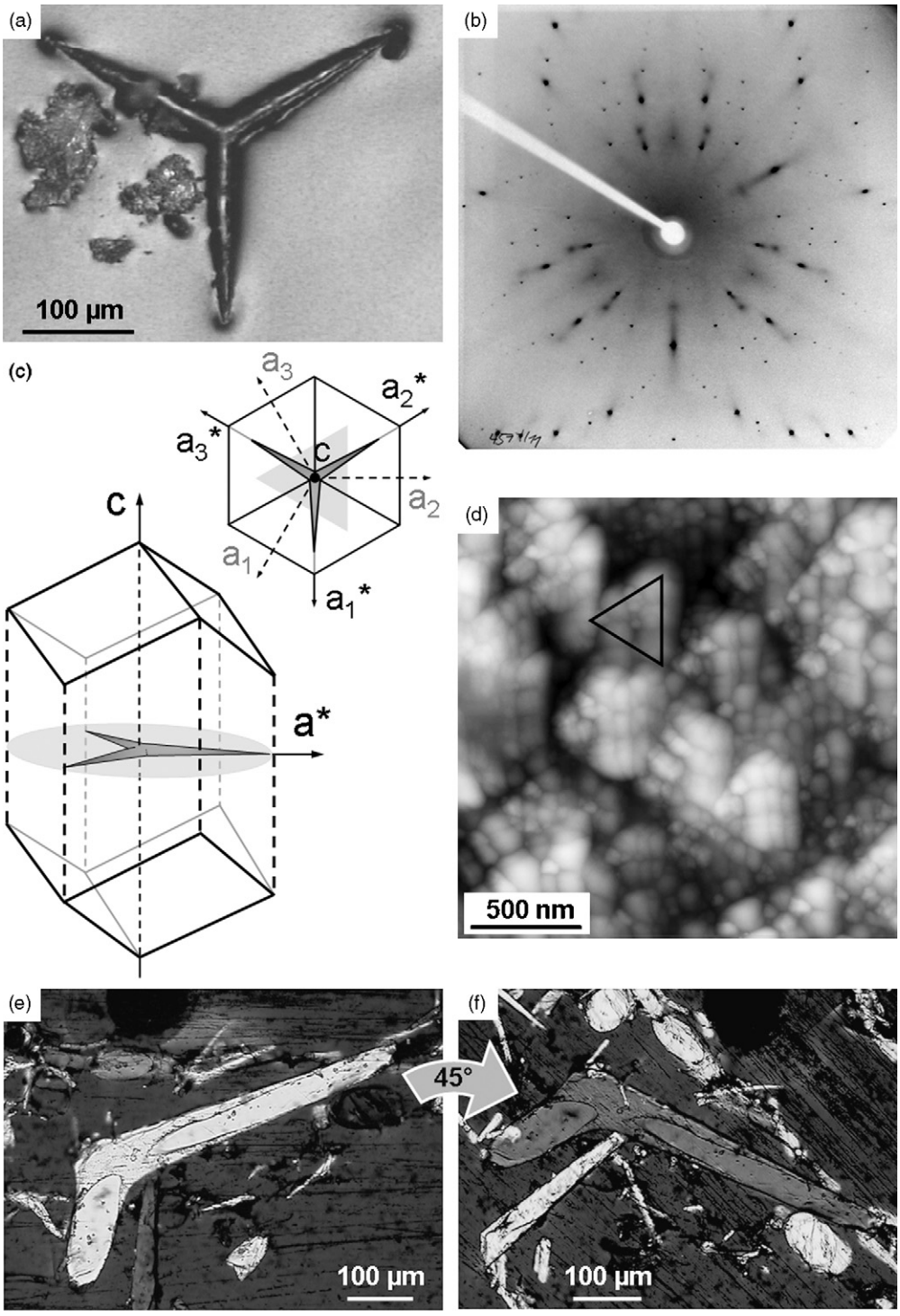

Fig. 3. Calcareous sponge spicules largely behave as calcite single-crystals (example: triactines of *Pericharax heteroraphis*). (a) Optical micrograph of a small regular triactine in reflected light. (b) X-ray diffraction Laue pattern confirms calcitic single-crystalline behaviour of the spicules; orientation as in (a), incident beam parallel to the *c*-axis. (c) Drawing of a spicule as in (a) in its crystallographic orientation in relation to a calcite $\{1\,0\,\bar{1}\,4\}$ rhombohedron and the crystallographic axes. (d) Triangular etch figures on a spicule surface in water are morphologically related to crystallography (compare (c)), despite the granular appearance of the material; spicule orientation as in (a–c) (AFM height image, height range ~40 nm). (e and f) Thin section of spicules in various orientations viewed in transmitted light with crossed polarizers; rotation by 45° from bright orientation to extinct orientation indicate single-crystallinity. Images (a–c, e and f) reproduced and partly modified from Sethmann et al. (2006).

other hand, impurities, especially the often high magnesium contents (5.2–18 mol% $MgCO_3$ in different samples; Jones and Jenkins, 1970; Aizenberg et al., 1995a; Sethmann et al., 2006), reduce the thermodynamic stability of the spicules in low-Mg aqueous solutions compared to the stability of pure calcite (e.g., Berner, 1975; Morse and Arvidson, 2002).

An investigation of calcarean spicules for their stable isotope values by Wörheide and Hooper (1999) yielded distinctive

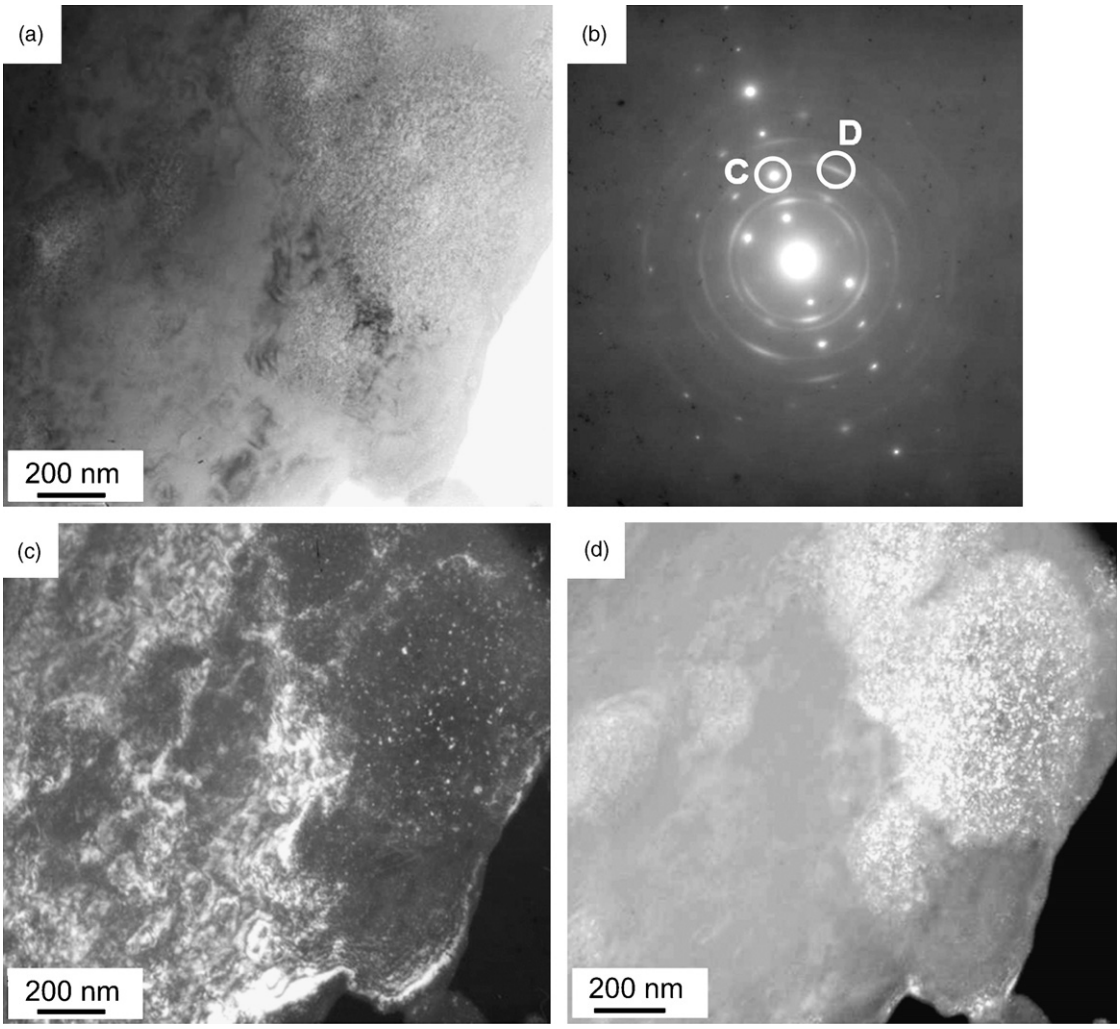

Fig. 4. Electron diffraction reveals locally differential crystallographic alignment in the spicule material (example: triactine of *Pericharax heteroraphis*). (a) TEM bright field image of the spicule material. (b) Electron diffraction pattern of the material; incident beam direction almost perpendicular to the $(\bar{1}\,0\,1\,\bar{4})$ plane of the predominant calcite 'single-crystal'. C, diffraction spot of the regular pattern selected for (c); D, streaked diffraction spot of the irregular pattern selected for (d). (c) Dark field image of the same area as in (a), obtained by using the regular diffraction spot C in (b), highlighting correspondingly diffracting areas of the predominant 'single-crystal'. (d) Dark field image of the same area as in (a), obtained by using the irregular diffraction spot D in (b), highlighting correspondingly diffracting areas that are misaligned with respect to the predominant 'single-crystal'. Figure reproduced from Sethmann et al. (2006).

stable isotopic compositions for the calcarean subclasses, respectively: negative δ^{13}C values and δ^{18}O values between −1.39 and −2.39 for Calcinea, and positive δ^{13}C values and δ^{18}O values between −0.28 and −1.41 for Calcaronea (in ‰ relative to PDB, Peedee belemnite standard). The different δ^{13}C ranges were attributed to different (yet unknown) cellular and/or subcellular mechanisms of biocalcification in the two subclasses that result in different processes of carbon isotope fractionation, as previously proposed by Reitner (1992). The processes that caused the observed differential oxygen isotope fractionation remained unclear.

3.2. Intraspicular mineral ultrastructures

Apart from the nanometre-scaled semicoherent cluster structure mentioned above, etch experiments on cross-sections clearly revealed an ultrastructure of concentric lamination around the axes of the actines of some spicules, which is often hardly visible on fresh fracture surfaces without etching (Fig. 5c and d) (Grant, 1826b; Haeckel, 1872; von Ebner, 1887; Jones and James, 1972; Ledger and Jones, 1991). An early controversial discussion about the existence of this lamellar structure (see Haeckel, 1872) was mediated by von Ebner (1887) in stating that it occurs only in large spicules, while small ones with thin actines lack this ultrastructure. von Ebner explains the formation of the lamellae with a periodic change of materials, concerning the content of impurities and/or defect structures. He suggested that concentric etch furrows and deep etch pits in the axial region of the acitines correspond to areas with defective or less pure calcite that dissolves more rapidly than pure and well-crystallized calcite. An electron microprobe investigation of *Leuconia nivea* spicules by Jones and James (1969), though, yielded no correlation of magnesium, strontium, and sulphur impurities with the lamellar structure, since the element distributions appeared to be homogeneous, which, however, could have been due to insufficient spatial or

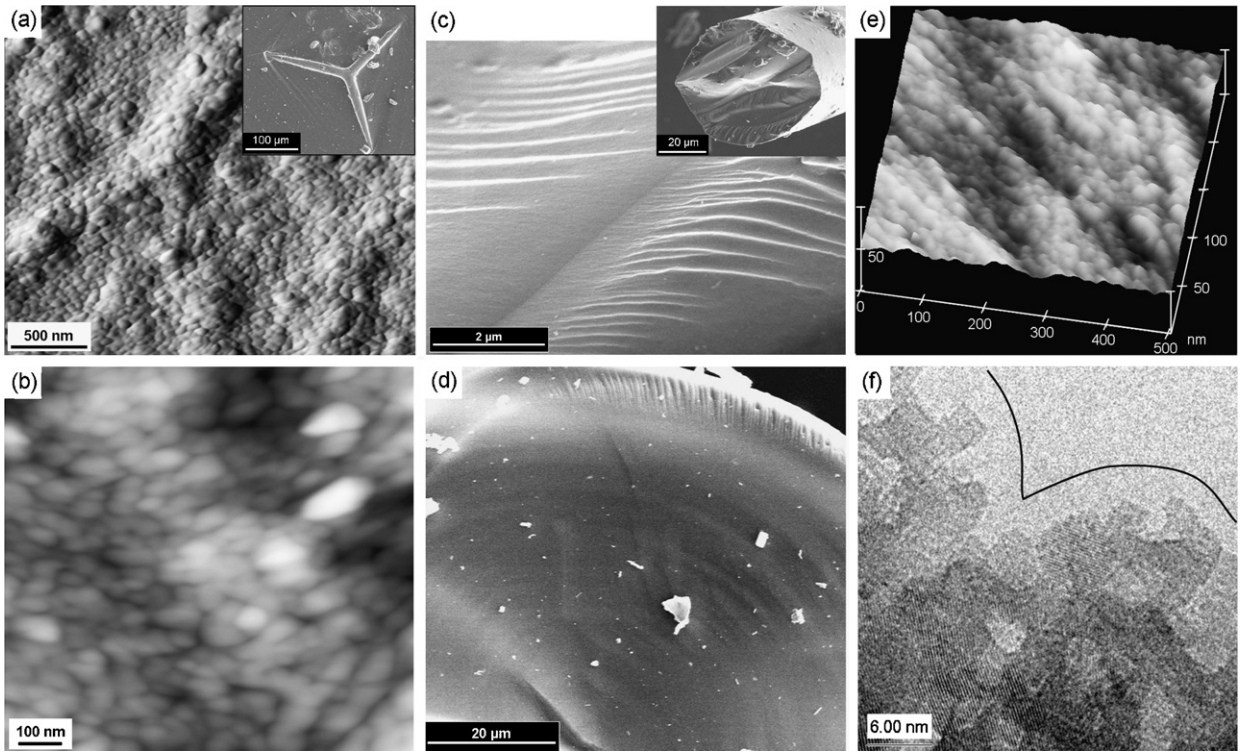

Fig. 5. Calcareous sponge spicules possess unusual material properties (example: triactines of *Pericharax heteroraphis*). (a) Granular surface structure with low relief of an actine of a regular triactine with rounded morphology (AFM deflection image; inset: complete spicule, field-emission SEM). (b) Nano-granular structure on a naturally grown spicule surface (AFM height image, height range ~20 nm). (c) Fractured actine showing a conchoidal fracture pattern (inset and magnified detail: field-emission SEM). (d) Fractured actine revealing a concentric layer pattern (field-emission SEM). (e) Conchoidal fracture surface revealing a nano-cluster structure of the spicule material (AFM). (f) High-resolution TEM reveals partly aligned and coherent crystal domains, the boundaries of which guide propagating fractures and deflect them from crystal cleavage planes. The line relates the angular fracture morphology to that displayed in (e). Insets of (a) and (b), and image (f) reproduced and modified from Sethmann et al. (2006).

analytical resolution. TEM images of spicules of a *Scypha* Gray, 1821 (= *Sycon*) species by Travis (1970) show quite convincing evidence for periodic intercalation of mechanically stronger mineralized layers. Lamellar shrinkage cracks, observed by scanning electron microscopy (SEM), suggested natural water content or organic matter accumulations in certain lamellae (Jones and James, 1972).

Differential thermal and dissolution stabilities of materials in triacines of a *Clathrina* species, as supported by synchrotron X-ray diffraction and infrared spectroscopy, revealed a layered substructure of two different, spatially separate $CaCO_3$ phases in the actines of these special spicules: An axial core of Mg-calcite is mantled by a layer of hydrated ACC and apparently by an additional thin calcitic coating at the spicule surface (Fig. 6; Aizenberg et al., 1996a, 2003a).

4. Organic components of the spicules

4.1. Spicule sheath and putative axial filament

Every single $CaCO_3$ spicule in calcareous sponges is enveloped by a tightly attached sheath (Fig. 7a and b). Due to the fact that these sheaths are quite easily recognizable, at least in the case of large mature spicules, their presence has been reported for many species of Calcarea. Based on observations by optical microscopy, Haeckel (1872) decidedly states that the sheath is formed not before the spicule formation is completed, while Minchin (1898) observed synchronous formation of spicules and the sheaths, the latter becoming more discernable in the course of spicule growth. More recent TEM studies by Jones (1967) and Ledger and Jones (1977) confirm the presence of a very thin membraneous sheath that envelopes the spicules of *Leucosolenia complicata* Montagu, 1818, already during their development. Therefore, the materials for spicule growth must pass through the sheath membrane to reach the site of mineral deposition. In the course of spicule development the tightly attached membrane becomes progressively displaced and dilated by the progressing mineral surface of the growing spicule (Ledger and Jones, 1977). Upon exposition to the open system of extracellular matrix (mesohyl), mature spicules acquire thicker protecting sheaths by accumulation of mostly thin, mesohyl-derived collagenous fibrils (Fig. 7b) that often link two spicules together (Jones, 1967; Ledger, 1974). Detailed descriptions of different types of collagen fibres and fibrillar network structures of the spicule sheaths of a *Scypha* (= *Sycon*) species are given by Travis et al. (1967) and of *Sycon* and *Leucandra* Haeckel, 1872, species by Ledger (1974).

It has been discussed controversially for a long time whether the actines of calcareous sponge spicules contain a central canal with an organic axial filament, comparable to the filaments that are undoubtedly and invariably present in all siliceous sponge

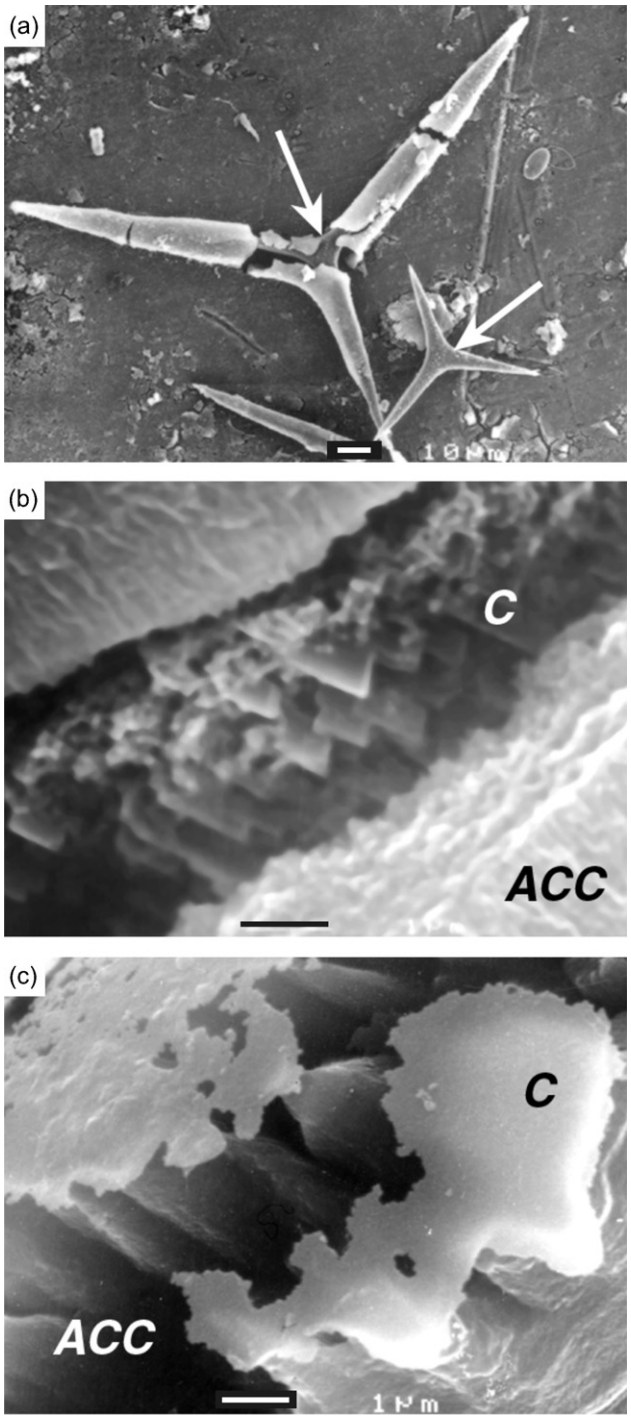

Fig. 6. Chemical treatment of triactine spicules of a *Clathrina* species reveals a combination of two mineral phases. (a) A heated spicule shows the calcitic cores (indicated by arrows) covered by a layer of ACC; scale bar 10 µm. (b) High magnification of a partially KOH-etched spicule reveals irregularly shaped deep etch pits in the ACC layer and regular etch figures on the surface of the calcitic core (C); scale bar 1 µm. (c) The same treatment reveals a thin calcitic outer layer (C) covering the ACC layer; scale bar 1 µm. Figure: Copyright 2003, from Aizenberg et al. (2003a). Reproduced by permission of Taylor & Francis Group, LLC, http://www.taylorandfrancis.com.

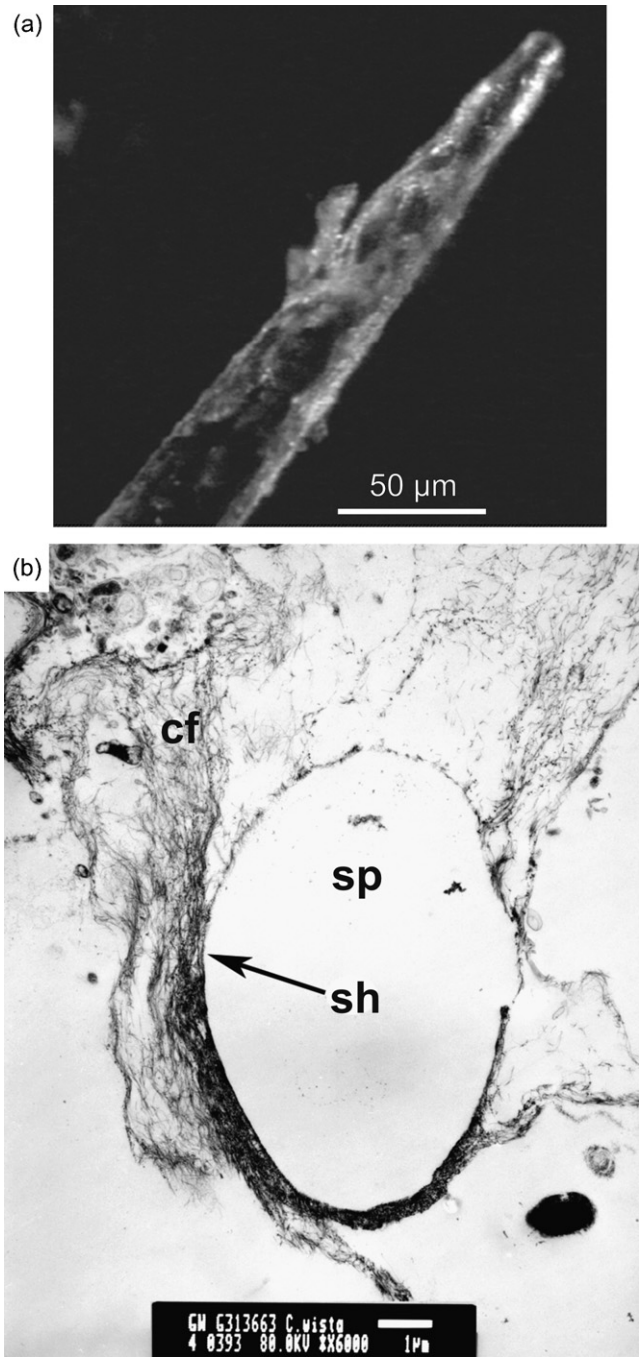

Fig. 7. Calcareous sponge spicules are enveloped by an organic sheath. (a) Optical micrograph of one tip of a triactine from *Pericharax heteroraphis* with the sheath partially detached. (b) *Clathrina wistariensis* Wörheide and Hooper, 1999: TEM micrograph of a spicule (sp; dissolved during preparation for TEM), which is surrounded by a sheath (sh; arrow) and mesohyl-derived collagenous fibres (cf). Scale bar 1 µm.

spicules (see Section 7.1). Grant (1826a,b) and Haeckel (1872) agree in their opinion that a central canal with a very thin filament exists in calcareous spicules, which in many cases can easily be overlooked. However, Haeckel also gives an overview of consenting as well as contrary opinions of other early investigators. With an optical microscope a linear feature had been observed in the actine axes of unprepared clear spicules, which turned brownish upon strong heating. This feature was interpreted as an organic filament that had turned into coal. Fractured actines, however, never showed a clearly discernable central canal or even a protruding filament. For this reason von Ebner (1887) dismissed the existence of an organic filament,

and he explained the linear axial features in the actines as an optical effect of light refraction by the spicule. Furthermore, he puts forward that minor constituents of the spicule material, such as water, evaporate upon heating and form cloudy gas inclusions, which account for the browning in transmitted light. The controversial discussion was further nourished by the finding of filamentous organic residues after dissolution of spicules that could be stained similar to the spicule sheath (reviewed by Minchin, 1909). After this discussion had continued for decades, Jones (1967) and Ledger and Jones (1977) finally have unequivocally shown in their TEM studies on *Leucosolenia complicata* and *Sycon ciliatum* Fabricius, 1780, that upon spicule decalcification no central filament remains as a coherent organic structure. The putative organic filament, revealed by $CaCO_3$ dissolution experiments, was demonstrated to be in fact identical with the contracted spicule sheath (Ledger and Jones, 1991). It is now generally accepted that calcareous sponge spicules do not contain a coherent organic axial filament.

4.2. Intraspicular organic matrix

Haeckel (1872) and others were convinced from their observations of conchoidal fracture surfaces and from heating and dissolution experiments that the calcareous mineral phase of the spicules was intimately associated with variable but always small amounts of dispersed or loosely connected organic material. They thought that this organic material influences the fracture behaviour of the spicule calcite, and that it could be charred by strong heating and dissolved in NaOH and KOH solutions. Haeckel (1872) noted that the amount of incorporated organic substance, which he termed ‘spiculin’, appears to be dependent on the morphological type of the spicule. Also Weinschenk (1905), comparing calcareous sponge spicules with non-biogenic calcite, decidedly attributed many of the differential properties of spicules to the presence of a finely dispersed organic matrix incorporated by the calcium carbonate.

Early TEM images of large spicules of a *Scypha* (= *Sycon*) species by Travis (1970) showed a system of very faint lines that were claimed to represent hierarchical organic matrix compartments, consisting partly of collagen fibrils. However, these results could not be reproduced by Ledger and Jones (1991), who doubted especially the existence of intra-spicular collagen and furthermore attribute the putative compartment walls to preparation and imaging artefacts. These authors stated that TEM investigations for an intracrystalline organic matrix of calcareous spicules yielded no clear evidence on stained samples, possibly due to the inevitable decalcification during the staining process.

In a different approach Aizenberg et al. (1996b) proved the presence of proteinaceous macromolecules incorporated in the calcitic bulk of spicules from *Clathrina*, *Kebira*, and *Sycon* species (0.07–0.1 wt%) by extraction and amino acid analyses. Referring to crystallographic data of coherences lengths, formerly obtained by synchrotron X-ray diffraction measurements (Aizenberg et al., 1995a,b), they inferred that the intracrystalline macromolecules form inclusions preferentially at domain boundaries corresponding to certain molecule-specific lattice planes. Recently, Sethmann et al. (2006) succeeded in imaging the distribution of an organic substance incorporated in the calcite of *Pericharax heteroraphis* spicules on a nanometre scale. This has been done by mapping the differential carbon content of the calcium carbonate and the organic substances by energy-filtering TEM on unstained samples (Fig. 8). A comparison of the carbon distribution maps with the corresponding calcium distribution and high-resolution TEM images shows that the organic matrix molecules are indeed intercalated between calcite crystal domains. However, at least in the TEM-imaged areas, the organic matrix distribution at boundaries of very small crystal domains was much denser than previously proposed by Aizenberg et al. (1996b), who assumed average minimum distances, i.e., protein-induced crystal domain dimensions, of more than 100 nm (Fig. 2). On the basis of the TEM images by Sethmann et al. (2006) the assumption of preferential incorporation of

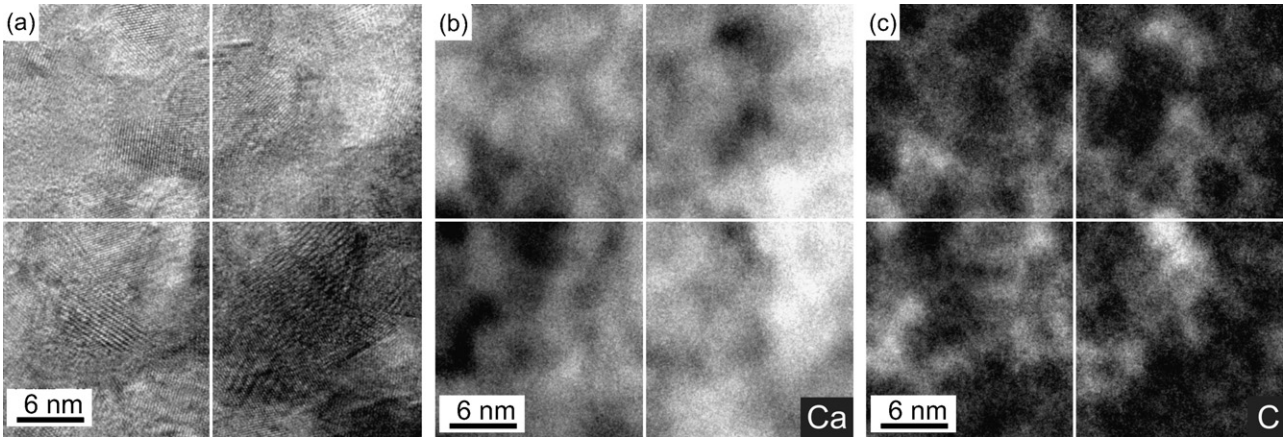

Fig. 8. Intracrystalline organic matrix in calcareous sponge spicules (example: *Pericharax heteroraphis*; crushed, uncoated sample). All images show the same sample area and are subdivided into four sectors as a guide to the eye: (a) high-resolution TEM reveals misaligned domains in the spicule calcite crystal. (b) Calcium-distribution map (energy-filtering TEM). (c) Carbon-distribution map (energy-filtering TEM). (b and c) Lighter shadings correspond to higher concentrations; note the negative correlation of Ca-enriched areas (representing $CaCO_3$) and C-enriched areas (representing the organic matrix).

macromolecules according to certain crystal planes can be neither confirmed nor dismissed. As suggested by Aizenberg et al. (1995b, 1996b), the amount and distribution of organic matrix material in the calcareous sponge spicules may vary with sponge species and spicule type.

The dispersed proteinaceous organic matrix in calcitic spicules is usually rich in aspartic acid (and/or asparagine) (Aizenberg et al., 1996b). In contrast, the ACC layers in spicules of a *Clathrina* species contain relatively little aspartic acid and are significantly enriched in glutamic acid (and/or glutamine), serine, glycine, and polysaccarides, compared to the calcitic cores of these spicules (Aizenberg et al., 1996a, 2003a). $CaCO_3$ precipitation experiments demonstrated that macromolecules, extracted from the amorphous layers, cause the formation and stabilization of ACC as granular aggregates, morphologically similar to the calcitic granular structures of the sponge spicules observed by Sethmann et al. (2006) (Figs. 3d and 5a, b and e). Hence, related formation mechanisms may be implied but are not proven.

5. Spicule formation

5.1. Cellular factors

In Calcarea, spicule formation takes place extracellularly in an intercellular cavity: specialized cells, the so-called sclerocytes, initially arrange to form a spicule primordium with their cell membranes tightly lining the growing spicule and separating it from the mesohyl (Fig. 9), as previously also documented partly by Jones (1967) for *Leucosolenia complicata* and to more extent by Ledger and Jones (1977) for *Sycon ciliatum* by TEM. During spicule growth sclerocytes secrete mineral and organic materials into the intercellular space, where calcium carbonate usually crystallizes as calcite. No storage or transport of mineralized $CaCO_3$ for spicule formation has been observed in sponge cells, which suggests that the sclerocytes constantly take up Ca^{2+} from the mesohyl, the ultimate ion source being the ambient seawater (Ledger and Jones, 1977). As these authors point out, the mechanism for ion accumulation and transport through the cells towards the mineralization site is not clear, but according to their observations vacuoles in sclerocytes appear to release non-mineralized material at the cell–spicule interface. However, the form in which the materials for spicule growth are secreted and the secretion mechanism itself remain largely unknown.

Each actine starts to grow out from the central nucleation point of the spicule (Weinschenk, 1905; Jones, 1954; Ledger and Jones, 1977), with each actine being formed by at least two sclerocytes for spicules with up to three actines (see Minchin, 1898 on species of *Clathrina*; Woodland, 1905 on species of *Sycon* and *Grantia* Fleming, 1828; Minchin, 1908 and Jones, 1954 on species of *Leucosolenia* Bowerbank, 1864; summary by Jones, 1970, and Ledger and Jones, 1977, on *Sycon ciliatum*). One of these sclerocytes, the 'founder cell', is responsible for the elongation of the spicule actine and moves outward from the origin in its growth direction, while others, the 'thickener cells', control its concentric thickening (Fig. 9; Minchin, 1898, 1908; Ledger and Jones, 1977). This concept of the cellular growth mechanism is supported by spicule growth patterns observed by Ilan et al. (1996), treating living sponges (*Sycon* sp.) with the fluorescent marker calcein. Spicules that continued growing after applying the dye were fluorescent at the tips of the actines, confirming radial outward growth from the centre. On the surfaces of some pre-existing (non-fluorescent) parts of actines fluorescent bands have been observed that could easily be removed by surface etching, which confirms the secondary thickening growth. Tetractines, probably pentactines, and possibly also the fossil heteractinid spicules are based on triactines. The formation of the additional actines is started by additional single sclerocytes, respectively, after the initial sclerocytes have started moving outwards from the centre while forming the first three actines, leaving space for the attachment of additional sclerocytes (Minchin, 1898; Jones, 1970; Rossi et al., 2006). Apical actine-forming sclerocytes may or may not divide during the growth process of tetractines, depending on the species (reviewed by Jones, 1970).

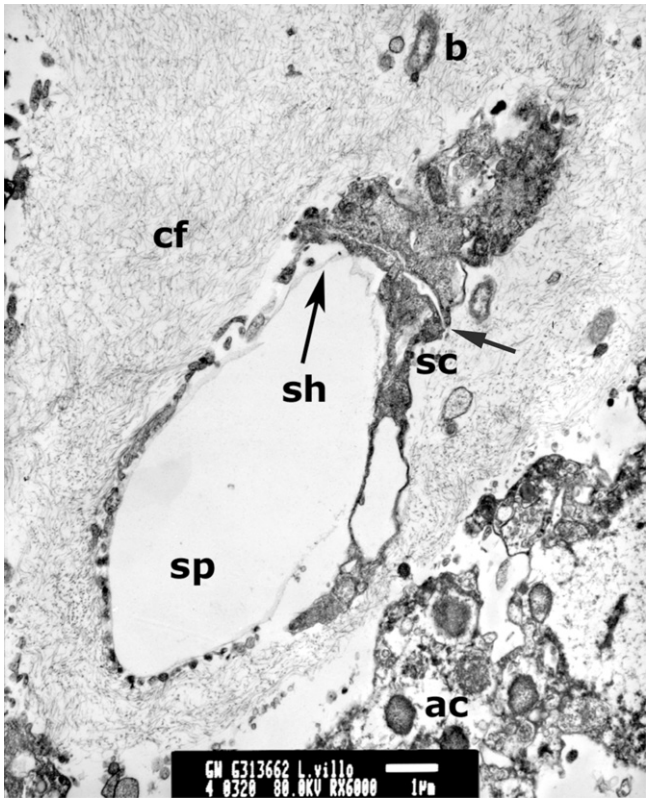

Fig. 9. *Leucetta villosa* Wörheide and Hooper, 1999: TEM micrograph of a small sclerocyte (sc) engulfing a young spicule (sp, dissolved during preparation for TEM). The spicule was covered with a thin sheath (sh; arrow). The mesohyl is filled with thin collagenous fibres (cf) and contains a few bacteria (b). An archaeocyte (ac) is visible in the lower right hand corner. A second cell, probably another sclerocyte, is next to the one engulfing the spicule (boundary between cells indicated by the narrow white space; short arrow). Scale bar 1 μm.

5.2. Mineral assembly and morphogenesis

Little is known about the initial determination of the spicule morphology and crystallographic orientation. Minchin (1898,

1908), Woodland (1905), Jones (1954), and Ledger and Jones (1977) observed that every single actine of a spicule is basically formed by two sclerocytes. Following this observation, it is understandable that the number and initial spatial arrangement of sclerocytes that form a spicule is predefining the number of spicule actines and possibly also their growth directions. Since each spicule behaves largely as a single-crystal of calcite in that the crystallographic orientation is much the same throughout the whole spicule, it is likely that crystal growth starts from a single calcite nucleus, heterogeneously formed in the primordium (e.g., Weinschenk, 1905; Jones, 1954; Ledger and Jones, 1977). An organic polyanionic 'template' probably defines the crystallographic orientation of the initial calcite nucleus and consequently that of the whole spicule (concept by Addadi et al., 1987; Heywood and Mann, 1994). After the initial nucleation event, the spicule grows probably almost exclusively by crystallization of new mineral material conformably to the crystal lattice of the pre-existing spicule calcite (e.g., Weinschenk, 1905; Jones, 1954; Aizenberg et al., 1996b; Sethmann et al., 2006), resulting on the whole in a single crystal individual or a well-aligned crystallite cluster.

The rounded morphologies of the spicules are very unusual, considering their single-crystalline properties, because single-crystals usually display distinct crystal faces. Organic and biological factors obviously play a role in the morphogenesis of the spicules. Therefore, Haeckel (1872) formulated his idea of 'biocrystals', which he considered as products of a compromise between the inorganic physical crystallization process and an organizing biological organic secretion activity. This concept takes into account that spicule actines are elongated according to defined crystallographic directions, despite their general lack of flat crystal faces. Weinschenk (1905) emphasises that the morphogenesis of rounded crystals requires continuous crystal growth with also continuous secretion of organic material, which becomes attached and occluded by the growing crystal, preventing the expression of the inorganic crystal form for the benefit of the organism. These ideas, expressed already a long time ago, are still valid to a great extent and form the basis for concepts of modern biomineralization research.

In spicules of *Pericharax heteroraphis* Sethmann et al. (2006) discovered a crystallographically largely aligned nano-cluster structure (Figs. 3–5) with an intercalated organic matrix (Fig. 8), which allows for different interpretations as to the process of spicule growth: they might grow either by oriented aggregation of preformed calcite particles, or preformed particles may initially consist of ACC, maybe temporarily stabilized by macromolecules, which then crystallize conformably to the pre-existing calcite substrate after their attachment (concepts and significance for biomineralization discussed by Aizenberg et al. (2003b), Politi et al. (2004), Cölfen and Antonietti (2005), Niederberger and Cölfen (2006), and Oaki et al. (2006)). A third possibility of nano-cluster crystal growth has been reported by Sethmann et al. (2005, in press) for calcite growth in the presence of polyaspartate. Under a gel-like thin film of polyaspartate, probably coagulated by Ca^{2+} or $CaCO_3$ molecules or nuclei, a calcite crystal grew as a crystallographically aligned nano-cluster. In that case the cluster blocks formed in place on the crystal surface. The porous gel-like structure of the covering film appeared to be important for cluster growth. A similar scenario may occur during spicule precipitation, since the proteins incorporated in the spicules are also rich in polyaspartate and have certainly been involved in the precipitation process (Aizenberg et al., 1996b). Previously, Aizenberg et al. (1995a,b) found a direct crystallographic-morphological correlation of orientation and elongation of macroscopic actines and the corresponding average crystal domains, probably formed under the influence of intercalated proteins. Interestingly and possibly relevant to the calcite nano-cluster formation, Ledger and Jones (1977) noted that the spicule materials, delivered by sclerocytes, must enter the intercellular spicule growth compartment by diffusion through the barrier of the sheath, which is tightly associated with the mineral surface. They assume that the sheath has a porous texture comparable with a thin gelatinous layer under which the crystal grows.

The elaborate crystal morphologies of spicules as physical structures may easily be modelled by a 'brick-by-brick' growth process as described above. The actual shaping, though, must arise from a presently unknown genetically determined control mechanism, involving controlled action of sclerocytes. Although the spicules form inside their sheaths, the rounded cylindrical or conical morphology of a spicule actine cannot be assigned to physical moulding by the tubular sheath, since the sheath does not represent a pre-formed, stiff mould. Instead, the sheath membrane becomes progressively displaced and extended by the mineral surface of the growing spicule (Ledger and Jones, 1977). The authors discuss an involvement of the sheath in spicule morphogenesis in so far as the increasing tension of the stretched sheath may exceed the crystallization pressure from the inside which then ceases crystal growth. More convincingly, however, the authors suggest that locally controlled supply of spicule growth materials by sclerocytes may regulate spicule morphology. Such a control method appears particularly efficient for growing elaborate structures, since the secreted spicule materials are probably deposited directly at the mineral–sheath interface after penetrating the sheath. However, if one accepts the nano-cluster structure and a corresponding growth mechanism together with locally controlled supply of growth materials, this growth process even less adequately explains spicule growth according to defined or even preferential crystallographic directions. The exact nature of the 'inorganic–organic compromise', as suggested by Haeckel (1872), is still puzzling.

The internal differentiation of large spicules into axial-concentric layers in the actines is obviously caused by differential material compositions or structures, and it can be assumed that the periodicity correlates to secretion intervals of the sclerocytes. This assumption is consistent with the spicule growth concept of concerted activity of a 'founder' and a 'thickener' sclerocyte for constructing each single spicule actine (Minchin, 1898, 1908; Woodland, 1905; Jones, 1954; Ledger and Jones, 1977). Ledger and Jones (1991) conclude that cyclical or discontinuous secretion is intrinsically caused or controlled by the involved cells, because the number of layers

in an actine is too high to correlate with a tidal or diurnal rhythm and/or sequential secretion by different cells, taking into account that the formation of a complete spicule takes no more than two days. Such rapid spicule formation was documented by in vivo-experiments on *Leucosolenia variabilis* Haeckel, 1870 (Jones, 1959, 1964), *Sycon* species (Jones and Ledger, 1986; Ilan et al., 1996), and *Clathrina cerebrum* Haeckel, 1872 (Bavestrello et al., 1993). Observed actine growth rates ranged from less than 1 μm to a maximum of more than 65 μm/h, depending on the sponge species, spicule type and size, stage of spicule development, and environmental conditions.

6. Mechanical properties of the spicules

Sponge spicules are elements of a skeleton that supports the sponge body, which means that they fulfil a mechanical function. Only in some calcarean taxa spicules coalesce to form a rigid framework ('Pharetronida'; orders Murrayonida Vacelet, 1981 [Calcinea] and Lithonida Vacelet, 1981 [Calcaronea]), but in the majority of taxa spicules are linked by more flexible organic fibres (e.g., Haeckel, 1872; Jones, 1967; Ledger, 1974) to form the tissue-supporting skeleton. However, a certain intrinsic balance of stiffness and toughness of the spicule material is doubtlessly advantageous. In this respect, the 'choice' of Calcarea to produce spicules invariably as single-crystals of high-Mg-calcite (>5 mol% $MgCO_3$; see Section 3.1) seems odd, since calcite crystals tend to break easily according to the $\{10\bar{1}4\}$ rhombohedral form with crystallographically equivalent cleavage planes in three different orientations. The less fragile $CaCO_3$ polymorph aragonite is also common in biomineralization (Lowenstam and Weiner, 1989), but the preference of Calcarea for Mg-calcite is probably a heritage from their evolutionary history, genetically fixed and biologically controlled by additives and/or organic templates for calcite-selective crystal nucleation.

However, calcarean species have overcome the anisotropic mechanical disadvantage of calcite crystals to some degree, since most fractured spicules show isotropic conchoidal fracture patterns (e.g., Haeckel, 1872; von Ebner, 1887; Weinschenk, 1905; Jones and James, 1972; Aizenberg et al., 1995b; Sethmann et al., 2006) (Fig. 5c), although more or less straight fractures according to the calcite cleavage planes also still occur in some cases (von Ebner, 1887; Aizenberg et al., 1995b). Early investigators have already attributed this unusual fracture behaviour and the remarkable toughness of the spicules to biologically induced structural modifications of the spicule material (e.g., Weinschenk, 1905). The layered internal construction implicates a periodic change of spicule materials, chemically and/or structurally, with differential physical properties, which apparently causes minor deflection of propagating fractures (von Ebner, 1887; Jones and James, 1972) (Fig. 5d). Differential fracture behaviour of clearly discernable layers parallel to the actine axis in spicules of *Scypha* (= *Sycon*) species is also demonstrated by TEM (Travis, 1970).

Also imperfections in the crystal coherence on smaller scale and a possibly intimately associated organic matrix have already been considered by early investigators as the cause of fracture deflection in the calcitic material (e.g., Haeckel, 1872; von Ebner, 1887; Weinschenk, 1905). TEM images by Travis (1970) show spicules of a *Scypha* (= *Sycon*) species, disintegrated upon ultramicrotome preparation into still largely oriented nanometre-scaled particles, that imply a pre-existing nano-granular material structure. These granule boundaries may have been coated by a dispersed proteinaceous organic matrix similar to those analyzed by Aizenberg et al. (1996b). In a recent study, Sethmann et al. (2006) have demonstrated by AFM and TEM techniques that in spicules of *Pericharax heteroraphis* fractures propagate by following the boundaries of clustered nanometre-scaled crystal domains (Fig. 5e and f) that were partly coated by organic matrix (Fig. 8). The intercalated organic matrix may have an additional toughening effect on the material by 'gluing' the clustered crystal domains together. Defect-guided fracture propagation, largely unaffected by crystal cleavage planes, produces fracture surfaces that are rough on a nanometre-scale (Fig. 5e and f) and show conchoidal patterns on larger scale (Fig. 5c). Apart from the nano-cluster-induced mechanical isotropy of spicule calcite, ACC that occurs in an internal layer of spicules of a *Clathrina* species (Fig. 6; Aizenberg et al., 1996a, 2003a) may also represent an adaptation for enhanced toughness by incorporating real isotropic material with no intrinsic cleavage planes instead of anisotropic crystals, as proposed by Addadi et al. (2003).

7. Structurally related biominerals

7.1. Siliceous sponge spicules

Spicular skeletons are common in all extant classes of Porifera, but in contrast to Calcarea with their calcitic spicules, all species of Hexactinellida and most of Demospongiae produce skeletal spicules of amorphous silica, also known as biogenic opal. In siliceous sponges, spicules occur in a vast morphological variety, much wider than in the Calcarea. Silica spicules are classified by their size into so-called megascleres (usually > 100 μm) and microscleres (usually < 50 μm). The function of the megascleres corresponds largely to that of the calcite spicules of the Calcarea in that they build up skeletal frameworks (e.g., Uriz et al., 2003a,b; Uriz, 2006). Demospongiae and Hexactinellida can be distinguished by the number of symmetry axes in the basic forms of their magascleres, being one to four axes for the Demospongiae (monaxons, triods/tripods, calthrops), and one and three axes for the Hexactinellida (monactines, diactines, hexactines). Silica megascleres may be connected by spongin fibres (as in most demosponges), but they can also fuse by cementation with an additional surrounding silica layer (hexactinellids) or interlock with one another ('lithistid' demosponges) to form rigid constructions (e.g., Uriz et al., 2003a,b; Uriz, 2006; Aizenberg et al., 2005). Microscleres are usually not part of rigid or spongin-connected skeletal frameworks but are dispersed in the sponge body (e.g., Uriz et al., 2003a,b), often reinforcing certain body parts, such as the cortex in species of *Geodia* Lamarck, 1815 (e.g., Hoffmann et al., 2002). Microscleres occur in the largest variety

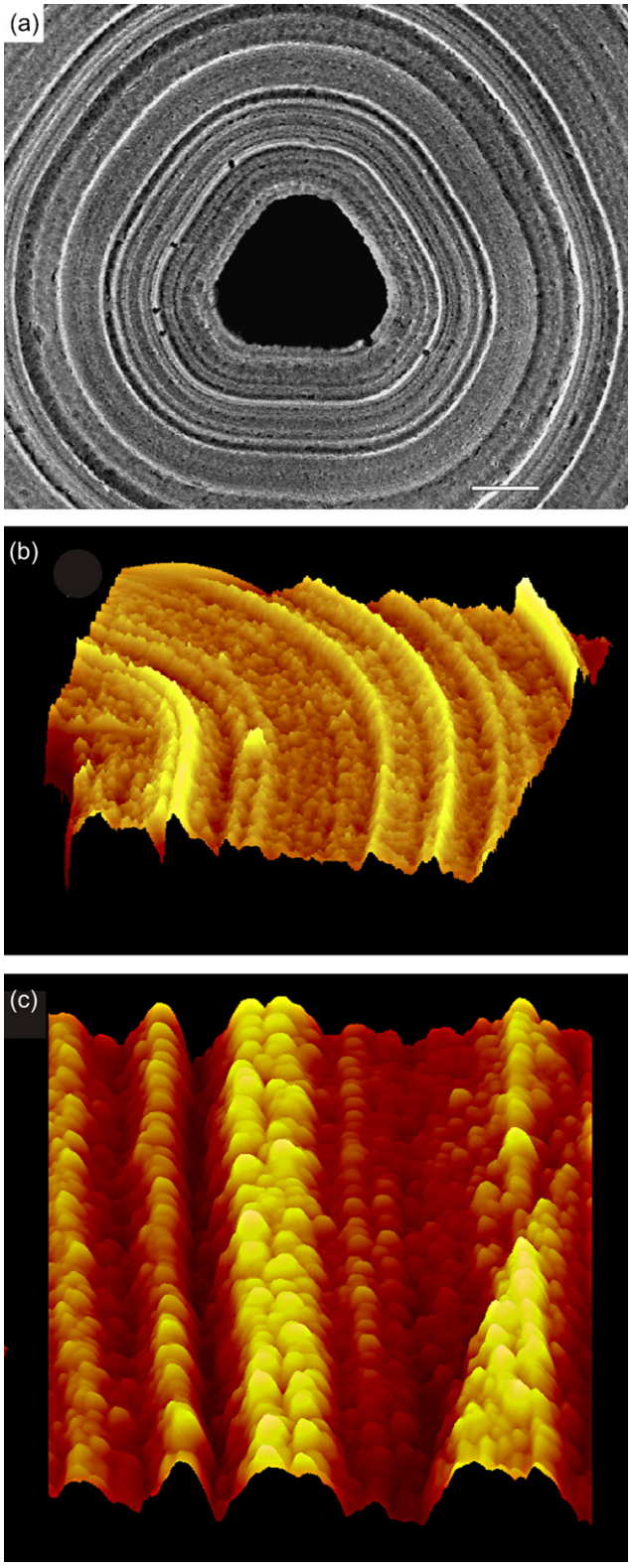

Fig. 10. Ultrastructure of siliceous sponge spicules (example: *Tethya aurantium* Pallas, 1766) as observed on sodium hypochloride-etched sections. (a) SEM of a spicule cross-section reveals concentric organization of the deposited silica as well as the central canal of the removed axial filament (scale bar 1 μm). (b) AFM surface plot of a spicule cross-section, illustrating concentric organization of deposited silica and the annular nanoparticulate substructure (scan size 3.8 μm, height data scale 275 nm). (c) AFM surface plot of a longitudinal-section revealing details of the annular nanoparticulate substructure (scan size 2 μm, height data scale 75 nm). Images reproduced from Weaver et al. (2003).

with species-specific morphologies, which makes them the predominant taxonomic tools (e.g., Hooper and Van Soest, 2002). However, under unfavourable environmental conditions microscleres may not be formed at all (e.g., Uriz and Maldonado, 1995). In the following, we will restrict the discussion to a brief structural comparison of the siliceous megascleres with the calcitic spicules, and for the sake of conciseness references will partly be limited to previously published reviews.

Silica spicules are initially formed intracellularly within vesicles of sclerocytes, and after reaching a certain size further spicule growth is accomplished extracellularly (Müller et al., 2006). All siliceous megascleres have a central canal with an organic axial filament as a common structure in every single spicule ray (e.g., Minchin, 1909; Uriz et al., 2003a,b) (Fig. 10a). The axial filament represents a composite of proteinaceous material and is formed prior to spicule silicification (Uriz et al., 2003a,b; Müller et al., 2006; Uriz, 2006). The axial filament determines the spicule morphology by serving as a core structure to which silica is subsequently attached during spicule growth (Weaver and Morse, 2003). Silica spicules show fine concentric laminations (Fig. 10), which suggests that the thickening process of the spicules takes place discontinuously (Schulze, 1904; Schwab and Shore, 1971; Uriz et al., 2000; Pisera, 2003; Sandford, 2003; Weaver and Morse, 2003; Weaver et al., 2003; Aizenberg et al., 2005). Nano-indentation experiments have demonstrated a much lesser stiffness of the silica material compared to industrial glass, and the concentric layers have been shown to provide differential mechanical properties (Woesz et al., 2006).

In hexactinellid spicules a lamination of higher order is much more developed, as especially demonstrated by their often foliated fracture pattern. Schulze (1904) already proposed that this fracture pattern is caused by intercalated organic laminae, an assumption recently demonstrated to be correct (Aizenberg et al., 2005). The organic laminae appear to act as internal mechanical sliding planes that enhance the fracture resistance of the spicules.

Siliceous spicules generally also show nano-granular ultrastructures as demonstrated by SEM (Pisera, 2003; Weaver et al., 2003; Weaver and Morse, 2003) and AFM (Fig. 10b and c; Weaver et al., 2003; Weaver and Morse, 2003; Aizenberg et al., 2005). These granules develop under the influence of silicatein (Weaver and Morse, 2003) and aggregate around the axial filament and later at the pre-existing spicule surface as concentric layers (Müller et al., 2006), forming the finely laminated ultrastucture of the spicule silicate (Pisera, 2003; Weaver et al., 2003; Aizenberg et al., 2005).

Apart from the organic laminae in hexactinellid spicules and the general occurrence of an axial filament, there seems to be no dispersed organic material incorporated in siliceous spicules. Siliceous spicules are not generally enveloped by a sheath as in

the Calcarea, but mature silica spicules usually become embedded in spongin fibres that connect the spicules to form a framework (Uriz et al., 2000, 2003). Recent reports about the presence of collagen as a scaffold for spicule formation in the hexactinellid *Hyalonema sieboldi* Gray, 1835 (Ehrlich et al., 2005) remain to be confirmed for other taxa.

Despite the difference in the basic materials, $CaCO_3$ (mainly as crystalline Mg-calcite) in Calcarea and SiO_2 (as amorphous opal) in Demospongiae and Hexactinellida, sponge spicules in general show conspicuous analogies in their precipitation mechanisms and construction patterns: Mineral material is assembled as nanostructural units around a central axis in concentric layers. The mineral precipitation takes place in the presence of proteinaceous substances and is probably controlled by them to some degree. In all cases, the mineral precipitation as nanostructural units enables the formation of specific elaborate spicule morphologies by locally controlled attachment of materials. These nano-granular structures enhance the materials toughness compared to their non-biogenic pure counterparts, Iceland spar (calcite) and silica glass, which provides additional fracture resistance to the skeletal frameworks. In hexactinellid spicules an additional strengthening effect is the intercalation of organic laminae, which may find a functional counterpart in the dispersed organic matrix in calcareous spicules. Structural correlations may be based on sub-cellular secretion mechanisms common to all Porifera.

7.2. Echinoderm skeletal elements

In Echinodermata, comprising the classes Echinoidea (sea urchins), Stelleroidea (starfish and brittle stars), Crinoidea (sea lilies and feather stars), and Holothuroidea (sea cucumbers), the skeletons consist of $CaCO_3$ in the calcite polymorph that contains considerable amounts of $MgCO_3$ (2–18.5 mol% in different species and environments; Weber, 1969, 1973; Magdans and Gies, 2004; Sethmann et al., 2005). We will focus largely on sea urchins as representatives for the whole group of the Echinodermata, since their skeletons are the most intensely investigated ones in this phylum. In these animals the mineralized test, a regular construction of macroscopically convex polygonal plates, contains and protects the inner organs, and a number of small ossicles form the feeding apparatus. Additionally, protective calcite spines are attached to the test of epibenthic sea urchins (i.e., those living on the surface of the seafloor). In all other groups of echinoderms skeletal elements fulfil corresponding functions of body support and protection.

A common feature of echinoderm skeletal elements is their unusual three-dimensional fenestrate structure, called stereom, with rounded smooth branches, called trabeculae, and an open pore system (Fig. 11a) that is filled with organic tissue in life animals. Despite their elaborate micromorphologies, each single skeletal element, plates, spines, and ossicles (except teeth), behaves largely as a calcite single-crystal, optically (e.g., von Ebner, 1887; Schmidt, 1924; Raup, 1959, 1962) as well as

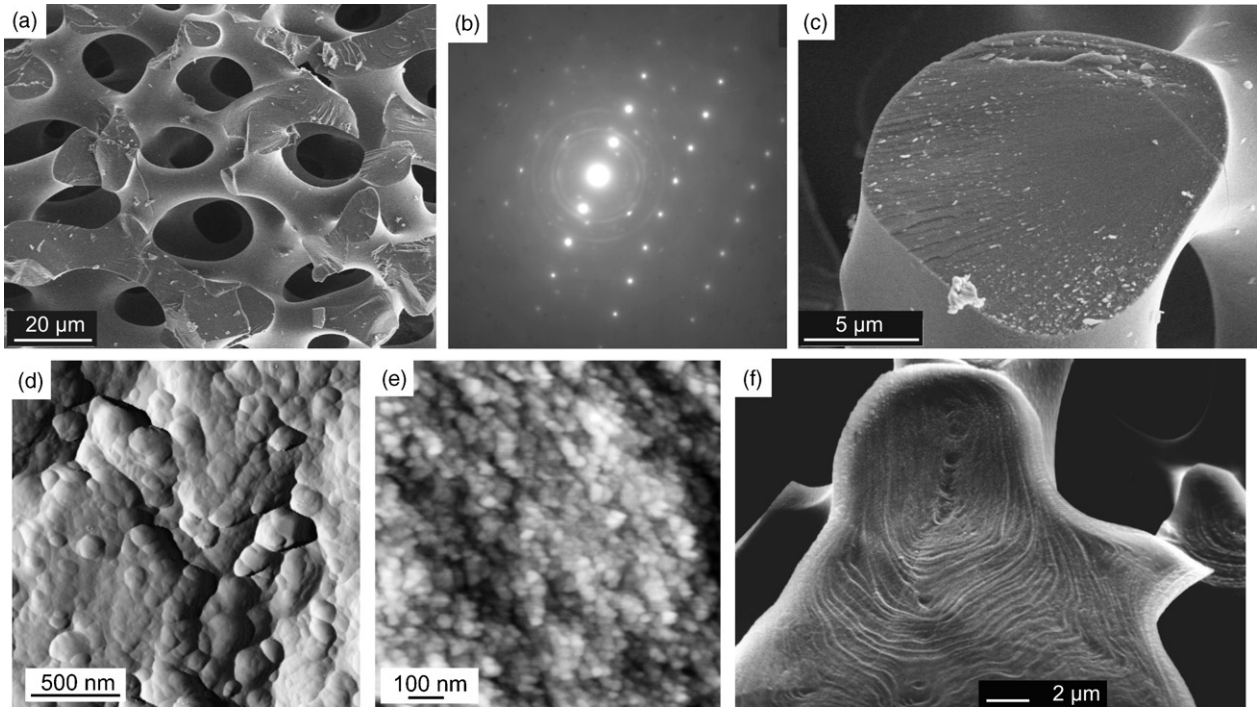

Fig. 11. Structure of calcitic sea urchin skeletal elements, (a–e) *Sphaerechinus granularis* Lamarck, 1816, (f) *Paracentrotus lividus* Lamarck, 1816. (a) SEM of the branched three-dimensional construction of a skeletal element with conchoidal fractures independent on crystallographic directions. (b) The electron diffraction pattern obtained from a small arbitrary fragment of a skeletal element reveals that misaligned crystal domains (ring pattern) are dispersed within the dominant crystallographically aligned calcite material; incident electron beam direction [4 0 1]. (c) Fracture surface of a trabecula at higher magnification (SEM). (d) Granular nanostructures on a naturally grown trabecular surface (AFM deflection image). (e) Fracture surface showing the conchoidal fracture pattern and the granular substructure (AFM height image, height range ~50 nm). (f) SEM of an EDTA-etched fracture surface of an immature sea urchin spine showing the mineral deposition lines. Image (a) reproduced and modified from Sethmann et al. (2005). Image (f) from Weiner and Addadi (1997). Reproduced by permission of The Royal Society of Chemistry.

in X-ray diffraction (e.g., Donnay and Pawson, 1969; Nissen, 1969; Sethmann et al., 2005) and electron diffraction (Fig. 11b; also Travis, 1970). Minor crystal domains in the skeletal elements are, however crystallographically misaligned (see secondary spot and ring pattern in Fig. 11b). In addition to this elaborate micromorphology, the calcitic single-crystalline appearance of the skeletal elements seems to be contradicted by their often nearly isotropic fracture behaviour, not typical for calcite crystals (e.g., Towe, 1967; Nissen, 1969; Aizenberg et al., 1997; Sethmann et al., 2005, in press) (Fig. 11a and c). (Towe, 1967; O'Neill, 1981) interpreted the single-crystalline-appearing skeletal elements as well aligned polycrystalline aggregates, based on SEM images on natural and fracture surfaces. Towe (1967) furthermore proposed that initially non-coherent crystallites coalesce during a maturation process. Travis (1970) observed disintegrated but crystallographically still aligned nano-granular structures in ultramicrotomed samples by TEM. High-resolution TEM observations of semicoherent crystal domains by Blake et al. (1984) and Tsipursky and Buseck (1993) arbitrate between single- and polycrystal concepts. Synchrotron X-ray diffraction data indicate a defect structure that subdivides the crystals into sub-micrometre-sized domains (Berman et al., 1993; Aizenberg et al., 1997). AFM images of a nano-cluster structure in sea urchin skeletal material imply the presence of semicoherent crystal domains of about 20–50 nm in size at maximum (Sethmann et al., 2005) (Fig. 11d and e). Aizenberg et al. (1997) proved that sea urchin spines contain small amounts (<0.1 wt%) of polyanionic proteins that were proposed to be intercalated at crystal defects between crystal domain boundaries. This proposition was recently confirmed by the TEM work of Oaki and Imai (2006). The organic inclusions and/or the crystal defects with which they are associated are thought to cause the enhanced toughness of the calcitic material and its conchoidal fracture pattern by dissipating mechanical stress and deflecting propagating fractures from the calcite cleavage planes (Smith, 1990; Weiner et al., 2000; Sethmann et al., 2005; Oaki and Imai, 2006), as demonstrated in Fig. 11e.

O'Neill (1981) as well as Weiner and Addadi (1997) report on layered growth structures in trabeculae of echinoderm skeletal elements (Fig. 11f), which suggest episodic discontinuous attachment of skeletal materials. Nano-granular structures on the growth surfaces of the skeletal elements, as revealed by AFM (Fig. 11d), suggest that crystal growth takes place in a 'brick-by-brick' pattern, either with the 'bricks' being attached as pre-formed probably amorphous particles (cf., Cölfen and Antonietti, 2005; Niederberger and Cölfen, 2006; Oaki et al., 2006), or with the 'bricks' growing in place, maybe from a precursor phase, under the influence of organic polyanions (Sethmann et al., 2005). Indeed, sea urchin calcite is known to form via a protein-stabilized ACC precursor within cavities chemically controlled by the enclosing cells (Politi et al., 2004). This process of skeleton formation in adult sea urchins corresponds to the formation of the larval spicules, for which Decker et al. (1987) and Beniash et al. (1999) observed intracellular pre-accumulation of ACC particles inside vesicles that are proposed to be involved in the spicule formation. During the formation of sea urchin larval spicules and adult skeletal elements protein-stabilized ACC precursor material gradually transforms into calcite, probably by crystallization conformable to a pre-existing calcite substrate (Beniash et al., 1997; Aizenberg et al., 2003b; Politi et al., 2004). Since many of the crystals of a skeleton, especially the echinoid spines, show a specific relation between macromorphology and crystallography (von Ebner, 1887; Schmidt, 1924; Raup, 1959, 1962; Donnay and Pawson, 1969; Nissen, 1969; Aizenberg et al., 1997), controlled and oriented nucleation of a single initial calcite crystallite is required for the skeletal elements.

Locally controlled and site-directed attachment of amorphous material may enable the morphogenesis of the elaborate stereom (Sethmann et al., 2005; Oaki and Imai, 2006). During crystallization of the precursor material the associated organic matter may easily become intercalated as inclusions in between crystal domains. The resulting reduced brittleness of the material is certainly advantageous, since less $CaCO_3$ has to be secreted to gain the same fracture resistance as in massive normal calcite. Additionally, it may allow the echinoderms to reduce the weight of their skeletons for better motility without losing too much of their protective function. However, the question why such elaborate skeletal elements are produced as single-crystals in the first place remains unanswered, since the trabeculae apparently grow in random directions without taking advantage of crystallographically preferential growth directions.

Although Echinodermata are phylogenetically only very distantly related to the calcareous sponges, the similar ultrastructures of their skeletal elements are conspicuous. Each element behaves largely as a single-crystal of Mg-calcite with weakly discernable, concentrically layered internal structures, probably growth rings, which are composed of nanometre-scaled, crystallographically aligned domains with dispersed organic matrices intercalated in between the domain boundaries. In both cases this internal structure causes advanced mechanical properties of the skeletal materials. These similarities of the materials may point to similar precipitation processes. While sea urchin calcite is known to precipitate via an ACC precursor (Beniash et al., 1999; Aizenberg et al., 2003b; Politi et al., 2004), there is no evidence for such a material transformation process in calcareous sponges. In calcareous sponge spicules only stable hydrated ACC is known, and only in one case (*Clathrina* sp.; Aizenberg et al., 1996a), but there is also no reason to exclude a precipitation scenario via a transient phase that so far may not have been detected.

8. Final remarks

Structural and compositional aspects of calcareous sponge spicules have been discussed controversially by many different investigators. Such controversies are not necessarily caused by inaccurate observations and interpretations, but in many cases they may arise from accurate observations on different materials, i.e., different spicule types from the same sponge

species, or spicules from different species. Within the common structural and compositional principles the possible occurrence of a certain variety of materials and patterns must be taken into account. Not all findings necessarily apply for the calcitic spicules in general.

A limited number of $CaCO_3$ biominerals is known to contain stable ACC or to form via transient ACC phases. However, the increasing number of ACC observations reported in biomineralization research suggests that ACC may be more common than is known so far and may have been overlooked due to the difficulty of detecting the amorphous phase if associated with crystalline $CaCO_3$ (Addadi et al., 2003). It would thus not come as a surprise, if sponge spicule calcite was found to be formed via an ACC transient phase, or if stable ACC was found in more spicule types than it has been to date.

Mineral assembly as nano-granular clusters, usually with small amounts of macromolecular organic substances intercalated between domain boundaries, is a widespread principle in biomineralization. This principle is applied in the skeletogenesis of many invertebrate animals, not only in the calcareous and siliceous sponge spicules and echinoderm skeletons, but also in various calcite and aragonite crystals of mollusc shells (Dauphin, 2001, 2003; Rousseau et al., 2005) and polycrystalline skeletons of scleractinian corals (aragonite) (Stolarski and Mazur, 2005), and octocorals (Mg-calcite) (Dauphin, 2006). The formation of these nanostructures is not well understood and may be achieved in different ways, but associated organic matrices might play an important role in biomineral nano-cluster precipitation (Sethmann et al., 2005; Rousseau et al., 2005). Apart from enabling complex crystal morphologies, another advantage of growing skeletal elements as nano-clustered semicoherent single-crystals, structural intermediates between perfect single-crystals and polycrystalline assemblies, seems to be a resulting enhancement of mechanical properties. This enhancement may be demonstrated by the fact that these intermediate materials are mechanically superior to the structural end-members of materials: polycrystalline coral skeletons with only little strength and elasticity (Wainwright et al., 1975) and non-biogenic pure calcite crystals that fracture easily according to their perfect cleavage planes.

Ultrastructural similarities of biominerals in different (only distantly related) taxa alone do not provide sufficient criteria to identify them as developmentally homologous structures. Precipitation of minerals as nano-granular structures seems to be a part of the biological mineralization-control mechanism. This nano-cluster formation is certainly caused by mineral-organic interactions, but the involved organic substances and exact physiological and regulatory processes are not well characterized and may vary to a great extent between different minerals and in different taxa. However, if these granular precipitation processes in various taxa, from sponges to echinoderms, share underlying genetic regulatory and control mechanisms, then parts of such a shared molecular mechanism for cation transport or prevention of uncontrolled mineralization were also present in the metazoan ancestor. However, evidence for such conserved mechanisms is still lacking, although some homologies between certain molluscan (Weiss et al., 2001) or sea urchin (Ettensohn et al., 2003) and vertebrate matrix proteins have already been postulated. Ettensohn et al. (2003), for example, found homologies of their sea urchin Sp/LvAlx1 protein, which is an essential component of the gene network that controls downstream genes required for biomineralization, with members of the vertebrate Cart1/Alx3/Alx4 protein family. Members of this gene family have been implicated to be instrumental in the formation of the limb skeleton and the neural crest-derived skeleton of the face and neck in vertebrates. Further, there seems to be some fundamental underlying immunological similarity between macromolecules involved in vertebrate hydroxyapatite and invertebrate aragonite formation (i.e., molluscan nacre), because freshly ground nacre did not result in an immune response when injected into human jaw bones, but in fact stimulated bone regeneration (Marin and Westbroek, 1998). Coral skeletons are already used as bone implants with a similar (albeit weaker) effect on bone regeneration (Demers et al., 2002). Although bone, nacre, and coral skeletons are not homologous structures as such, parts of the complex underlying physiological machinery that controls biomineral formation, even on the nanoscale, probably is—a hypothesis strongly supported by the above mentioned results.

However, these homologous parts may have served a different function than biomineralization in the (non-skeletized) common ancestor of sponges, corals, molluscs, echinoderms and vertebrates, later being co-opted for producing biominerals when the necessity arose. This powerful hypothesis still awaits an expanded program of comparative geobiological research (Knoll, 2003). A simple, pre-existing ancestral system then presumably evolved into the diverse existing complexity seen from the ‘‘Cambrian Explosion’’ onwards (Kirschvink and Hagadorn, 2000). One major process by which complex biological systems evolve is by taking an existing genetic pattern that evolved for a certain function and duplicating it, linking it up differentially, and adapting it for a new role (e.g., Caroll et al., 2001). The nascent system is gradually debugged and improved through the process of random mutation and natural selection.

The occurrence of concentric lamination in different biomineral elements can, however, probably be attributed to a physical necessity of thickness-growth by discontinuous mineral deposition. In general, the cellular context of biomineral elements is more suitable as a basis for an identification of homologous structures than the ultrastructures of the inorganic precipitates themselves.

The crystallographic orientation of most skeletal elements should be of no importance for their function. Consequently, some calcitic single-crystalline skeletal elements show preferred growth directions consistent with physically preferable intrinsic crystal directions. Surprisingly many skeletal elements, though, show biologically preferred crystal growth directions different from those preferred in pure crystal growth systems. Such strong modifications of crystal growth may require a stronger biological control over mineral precipitation, but they are necessary for achieving certain biomineral morphologies in some cases. However, a detailed investigation

of such relationships between physicochemical crystal growth and the cellular and genetic control mechanisms is lacking so far. The oriented initial crystal nucleation as well as the morphogenesis in the course of nano-clustered crystal growth is undoubtedly genetically programmed and controlled, but the exact control and regulatory mechanisms still remain enigmatic. However, unravelling the genetic machinery underlying those mechanisms might provide pivotal insights into the evolution of biomineralized structures in metazoans.

Acknowledgements

We thank Ruth Hinrichs and Christine Putnis for support with TEM and field-emission SEM. We acknowledge James C. Weaver, Joanna Aizenberg, and Lia Addadi for kindly providing us with images and figures. This work benefited from funding by the German Research Foundation (DFG): project Pu153/6-1,2,3 in priority program SPP 1117, 'Principles of Biomineralization' (IS), and projects Wo896/3-1, /4-1,2 (GW).

References

Addadi, L., Moradian, J., Shay, E., Maroudas, N.G., Weiner, S., 1987. A chemical model for the cooperation of sulfates and carboxylates in calcite crystal nucleation: relevance to biomineralization. Proc. Natl. Acad. Sci. U.S.A. 84, 2732–2736.

Addadi, L., Raz, S., Weiner, S., 2003. Taking advantage of disorder: amorphous calcium carbonate and its roles in biomineralization. Adv. Mater. 15, 959–970.

Aizenberg, J., Albeck, S., Weiner, S., Addadi, L., 1994. Crystal–protein interactions studied by overgrowth of calcite on biogenic skeletal elements. J. Cryst. Growth 142, 156–164.

Aizenberg, J., Hanson, J., Ilan, M., Leiserowitz, L., Koetzle, T.F., Addadi, L., Weiner, S., 1995b. Morphogenesis of calcitic sponge spicules: a role for specialized proteins interacting with growing crystals. FASEB J. 9, 262–268.

Aizenberg, J., Hanson, J., Koetzle, T.F., Leiserowitz, L., Weiner, S., Addadi, L., 1995a. Biologically induced reduction in symmetry: a study of crystal texture of calcitic sponge spicules. Chem. Eur. J. 1, 414–422.

Aizenberg, J., Hanson, J., Koetzle, T.F., Weiner, S., Addadi, L., 1997. Control of macromolecule distribution within synthetic and biogenic single calcite crystals. J. Am. Chem. Soc. 119, 881–886.

Aizenberg, J., Ilan, M., Weiner, S., Addadi, L., 1996b. Intracrystalline macromolecules are involved in the morphogenesis of calcitic sponge spicules. Connective Tissue Res. 34, 255–261.

Aizenberg, J., Lambert, G., Addadi, L., Weiner, S., 1996a. Stabilization of amorphous calcium carbonate by specialized macromolecules in biological and synthetic precipitates. Adv. Mater. 8, 222–226.

Aizenberg, J., Muller, D.A., Grazul, J.L., Hamann, D.R., 2003b. Direct fabrication of large micropatterned single crystals. Science 299, 1205–1208.

Aizenberg, J., Weaver, J.C., Thanawala, M.S., Sundar, V.C., Morse, D.E., Fratzl, P., 2005. Skeleton of *Euplectella* sp.: structural hierarchy from the nanoscale to the macroscale. Science 309, 275–278.

Aizenberg, J., Weiner, S., Addadi, L., 2003a. Coexistence of amorphous and crystalline calcium carbonate in skeletal tissues. Connective Tissue Res. 44 (Suppl. 1), 20–25.

Bavestrello, G., Cattaneo-Vietti, R., Cerrano, C., Sarà, M., 1993. Rate of spiculogenesis in *Clathrina cerebrum* (Porifera: Calcispongiae) using tetracycline marking. J. Mar. Biol. Assoc. U.K. 73, 457–460.

Beniash, E., Aizenberg, J., Addadi, L., Weiner, S., 1997. Amorphous calcium carbonate transforms into calcite during sea urchin larval spicule growth. Proc. R. Soc. Lond. B 264, 461–465.

Beniash, E., Aizenberg, J., Addadi, L., Weiner, S., 1999. Cellular control over spicule formation in sea urchin embryos: a structural approach. J. Struct. Biol. 125, 50–62.

Berman, A., Hanson, J., Leiserowitz, L., Koetzle, T.F., Weiner, S., Addadi, L., 1993. Biological control of crystal texture: a widespread strategy for adapting crystal properties to function. Science 259, 776–779.

Berner, R.A., 1975. The role of magnesium in the crystal growth of calcite and aragonite from sea water. Geochim. Cosmochim. Acta 39, 489–504.

Bidder, G.P., 1898. The skeleton and classification of calcareous sponges. Proc. R. Soc. Lond. 64, 61–76.

Blake, D.F., Peacor, D.R., Allard, L.F., 1984. Ultrastructural and microanalytical results from echinoderm calcite: implications for biomineralization and diagenesis of skeletal material. Micron Microsc. Acta 15, 85–90.

Borojevic, R., Boury-Esnault, N., Manuel, M., Vacelet, J., 2002a. Order Baerida Borojevic, Boury-Esnault, Vacelet, 2000. In: Hooper, J.N.A., Van Soest, R.W.M. (Eds.), Systema Porifera. Guide to the Supraspecific Classification of Sponges and Spongiomorphs (Porifera), vol. 2. Plenum, New York, pp. 1193–1199.

Borojevic, R., Boury-Esnault, N., Manuel, M., Vacelet, J., 2002b. Order Clathrinida Hartman, 1958. In: Hooper, J.N.A., Van Soest, R.W.M. (Eds.), Systema Porifera. Guide to the Supraspecific Classification of Sponges and Spongiomorphs (Porifera), vol. 2. Plenum, New York, pp. 1141–1152.

Borojevic, R., Boury-Esnault, N., Manuel, M., Vacelet, J., 2002c. Order Leucosolenida Hartman, 1958. In: Hooper, J.N.A., Van Soest, R.W.M. (Eds.), Systema Porifera. Guide to the Supraspecific Classification of Sponges and Spongiomorphs (Porifera), vol. 2. Plenum, New York, pp. 1157–1184.

Botting, J.P., Butterfield, N.J., 2005. Reconstructing early sponge relationships by using the Burgess Shale fossil *Eiffelia globosa*, Walcott. Proc. Natl. Acad. Sci. U.S.A. 102, 1554–1559.

Boury-Esnault, N., Rützler, K., 1997. Thesaurus of sponge morphology. Smithsonian Contrib. Zool. 596, 1–55.

Caroll, S.B., Grenier, J.K., Weatherbee, S.D., 2001. From DNA to Diversity—Molecular Genetics and the Evolution of Animal Design. Blackwell Science, Malden, MA.

Cölfen, H., Antonietti, M., 2005. Mesocrystals: inorganic superstructures made by highly parallel crystallization and controlled alignment. Angew. Chem. Int. Ed. 44, 5576–5591.

Dauphin, Y., 2001. Nanostructures de la nacre des tests de céphalopodes actuels. Paläont. Z. 75, 113–122.

Dauphin, Y., 2003. Soluble organic matrices of the calcitic prismatic shell layers of two pteriomorphid bivalves. J. Biol. Chem. 278, 15168–15177.

Dauphin, Y., 2006. Mineralizing matrices in the skeletal axes of two *Corallium* species (Alcyonacea). Comp. Biochem. Physiol. Part A 145, 54–64.

Decker, G.L., Morrill, J.B., Lennarz, W.J., 1987. Characterization of sea urchin primary mesenchym cells and spicules during biomineralization *in vitro*. Development 101, 297–312.

Demers, C., Hamdy, C.R., Corsi, K., Chellat, F., Tabrizian, M., Yahia, L., 2002. Natural coral exoskeleton as a bone graft substitute: a review. BioMed. Mater. Eng. 12, 15–35.

Dohrmann, M., Voigt, O., Erpenbeck, D., Wörheide, G., 2006. Non-monophyly of most supraspecific taxa of calcareous sponges (Porifera, Calcarea) revealed by increased taxon sampling and partitioned Bayesian analysis of ribosomal DNA. Mol. Phylogenet. Evol. 40, 830–843.

Donnay, G., Pawson, D.L., 1969. X-ray diffraction studies of echinoderm plates. Science 166, 1147–1150.

Ehrlich, H., Hanke, T., Meissner, H., Richter, G., Born, R., Heinemann, S., Ereskovsky, A., Krylova, D., Worch, H., 2005. Nanoimagery and the biomimetic potential of marine glass sponge *Hyalonema sieboldi* (Porifera). VDI-Berichte 1920, 163–166.

Ettensohn, C.A., Illies, M.R., Oliveri, P., De Jong, D.L., 2003. Alx1, a member of the Cart1/Alx3/Alx4 subfamily of paired-class homeodomain proteins, is an essential component of the gene network controlling skeletogenic fate specification in the sea urchin embryo. Development 130, 2917–2928.

Finks, R.M., Rigby, J.K., 2004. Heteractinida. In: Kaesler, R.L. (Ed.), Treatise on Invertebrate Paleontology, Part E (Revised), Porifera, vol. 3. Geological Society of America & University of Kansas, Boulder, Lawrence, pp. 557–583.

Grant, R.E., 1826a. Observations and experiments on the structure and functions of the sponge. Edinb. Philos. J. 14, 336–341.

Grant, R.E., 1826b. Remarks on the structure of some calcareous sponges. Edinb. New Philos. J. 1, 166–170.

Haeckel, E., 1869. Prodromus eines Systems der Kalkschwämme. Jenaische Z. 5, 236–254.

Haeckel, E., 1872. Die Kalkschwämme. Verlag Georg Reimer, Berlin.

Heywood, B.R., Mann, S., 1994. Template-directed nucleation and growth of inorganic materials. Adv. Mater. 6, 9–20.

Hoffmann, F., Rapp, H.T., Zöller, T., Reitner, J., 2002. Growth and regeneration in cultivated fragments of the boreal deep water sponge Geodia barretti Bowerbank, 1858 (Geodiidae, Tetractinellida, Demospongiae). J. Biotechnol. 100, 109–118.

Hooper, J.N.A., Van Soest, R.W.M. (Eds.), 2002. Systema Porifera. Guide to the Supraspecific Classification of Sponges and Spongiomorphs (Porifera). Plenum, New York.

Ilan, M., Aizenberg, J., Gilor, O., 1996. Dynamics and growth patterns of calcareous sponge spicules. Proc. R. Soc. Lond. B 263, 133–139.

Jones, W.C., 1954. The orientation of the optic axis of spicules of *Leucosolenia complicata*. Q. J. Microsc. Sci. 95, 33–48.

Jones, W.C., 1955a. Crystalline properties of spicules of *Leucosolenia complicata*. Q. J. Microsc. Sci. 96, 129–149.

Jones, W.C., 1955b. The sheath of spicules of *Leucosolenia complicata*. Q. J. Microsc. Sci. 96, 411–421.

Jones, W.C., 1959. Spicule growth rates in *Leucosolenia variabilis*. Q. J. Microsc. Sci. 100, 557–570.

Jones, W.C., 1964. Photographic records of living oscular tubes of *Leucosolenia variabilis*. II. Spicule growth, form and displacement. J. Mar. Biol. Assoc. U.K. 44, 311–331.

Jones, W.C., 1967. Sheath and axial filament of calcareous sponge spicules. Nature 214, 365–368.

Jones, W.C., 1970. The composition, development, form and orientation of calcareous sponge spicules. Symp. Zool. Soc. Lond. 25, 91–123.

Jones, W.C., James, D.W.F., 1969. An investigation of some calcareous sponge spicules by means of electron probe micro-analysis. Micron 1, 34–39.

Jones, W.C., James, D.W.F., 1972. Examination of the large triacts of the calcareous sponge Leuconia nivea Grant by scanning electron microscopy. Micron 3, 196–210.

Jones, W.C., Jenkins, D.A., 1970. Calcareous sponge spicules: a study of Magnesian Calcites. Calcified Tissue Res. 4, 314–329.

Jones, W.C., Ledger, P.W., 1986. The effect of diamox and various concentrations of calcium on spicule secretion in the calcareous sponge *Sycon ciliatum*. Comp. Biochem. Physiol. 84A, 149–158.

Kirschvink, J.L., Hagadorn, J.W., 2000. A grand unifying theory of biomineralization. In: Bäuerlein, E. (Ed.), The Biomineralization of Nano- and Micro-Structures. Wiley-VCH, Weinheim, pp. 139–150.

Knoll, A.H., 2003. Biomineralization and evolutionary history. In: Dove, P.M., De Yoreo, J.J.,Weiner, S. (Eds.), Biomineralization. Reviews in Mineralogy & Geochemistry, vol. 54. The Mineralogical Society of America, Washington, DC, pp. 329–356.

Ledger, P.W., 1974. Types of collagen fibres in the calcareous sponges *Sycon* and *Leucandra*. Tissue Cell 6, 385–389.

Ledger, P.W., Jones, W.C., 1977. Spicule formation in the calcareous sponge Sycon ciliatum. Cell Tiss. Res. 181, 553–567.

Ledger, P.W., Jones, W.C., 1991. On the structure of calcareous sponge spicules. In: Reitner, J., Keupp, H. (Eds.), Fossil and Recent Sponges. Springer, Berlin, Heidelberg, pp. 341–359.

Lowenstam, H.A., Weiner, S., 1989. On Biomineralization. Oxford University Press, New York.

Magdans, U., Gies, H., 2004. Single crystal structure analysis of sea urchin spine calcites: systematic investigations of the Ca/Mg distribution as a function of habitat of the sea urchin and the sample location in the spine. Eur. J. Mineral. 16, 261–268.

Mann, S., 1983. Mineralization in biological systems. Struct. Bonding 54, 125–174.

Manuel, M., Borchiellini, C., Alivon, E., Le Parco, Y., Vacelet, J., Boury-Esnault, N., 2003. Phylogeny and evolution of calcareous sponges: monophyly of Calcinea and Calcaronea, high level of morphological homoplasy, and the primitive nature of axial symmetry. Syst. Biol. 52, 311–333.

Manuel, M., Borojevic, R., Boury-Esnault, N., Vacelet, J., 2002. Class Calcarea Bowerbank, 1864. In: Hooper, J.N.A., Van Soest, R.W.M. (Eds.), Systema Porifera. Guide to the Supraspecific Classification of Sponges and Spongiomorphs (Porifera), vol. 2. Plenum, New York, pp. 1103–1110.

Marin, F., Westbroek, P., 1998. A marriage of bone and nacre. Nature 392, 861–862.

Minchin, E.A., 1898. Materials for a monograph of the ascons. I. On the origin and growth of the triradiate and quadradiate spicules in the family Clathrinidae. Q. J. Microsc. Sci. 40, 469–588.

Minchin, E.A., 1908. Materials for a monograph of the ascons. II. The formation of spicules in the genus *Leucosolenia*, with some notes on the histology of the sponges. Q. J. Microsc. Sci. 52, 301–335.

Minchin, E.A., 1909. Sponge-spicules. A summary of present knowledge. Ergebnisse und Fortschritte der Zoologie 2, 171–274.

Morse, J.W., Arvidson, R.S., 2002. The dissolution kinetics of major sedimentary carbonate minerals. Earth-Sci. Rev. 58, 51–84.

Müller, W.E.G., Belikov, S.I., Tremel, W., Perry, C.C., Gieskes, W.W.C., Boreiko, A., Schröder, H.C., 2006. Siliceous spicules in marine demosponges (example *Suberites domuncula*). Micron 37, 107–120.

Niederberger, M., Cölfen, H., 2006. Oriented attachment and mesocrystals: non-classical crystallization mechanisms based on nanoparticle assembly. Phys. Chem. Chem. Phys. 8, 3271–3287.

Nissen, H.U., 1969. Crystal orientation and plate structure in echinoid skeletal units. Science 166, 1150–1152.

O'Neill, P.L., 1981. Polycrystalline echinoderm calcite and its fracture mechanics. Science 213, 646–648.

Oaki, Y., Imai, H., 2006. Nanoengineering in echinoderms: the emergence of morphology from nanobricks. Small 2, 66–70.

Oaki, Y., Kotachi, A., Miura, T., Imai, H., 2006. Bridged nanocrystals in biominerals and their biomimetics: classical yet modern crystal growth on the nanoscale. Adv. Funct. Mater. 16, 1633–1639.

Pickett, J., 2002. Order Heteractinida Hinde, 1887. In: Hooper, J.N.A., Van Soest, R.W.M. (Eds.), Systema Porifera. Guide to the Supraspecific Classification of Sponges and Spongiomorphs (Porifera), vol. 2. Plenum, New York, pp. 1121–1139.

Pisera, A., 2003. Some aspects of silica deposition in lithistid demosponge desmas. Microsc. Res. Tech. 62, 312–326.

Politi, Y., Arad, T., Klein, E., Weiner, S., Addadi, L., 2004. Sea urchin spine calcite forms via a transient amorphous calcium carbonate phase. Science 306, 1161–1164.

Raup, D.M., 1959. Crystallography of echinoid calcite. J. Geol. 67, 661–674.

Raup, D.M., 1962. The phylogeny of calcite crystallography in echinoids. J. Paleontol. 36, 793–810.

Reitner, J., 1992. "Coralline Spongien". Der Versuch einer phylogenetisch taxonomischen Analyse. Berliner Geowissenschaftliche Abhandlungen, Reihe (E). Palaeobiologie 1, 1–352.

Rossi, A.L., Farina, M., Borojevic, R., Klautau, M., 2006. Occurrence of five-rayed spicules in a calcareous sponge: *Sycon pentactinalis* sp. nov. (Porifera: Calcarea). Cah. Biol. Mar. 47, 261–270.

Rousseau, M., Lopez, E., Stempflé, P., Brendlé, M., Franke, L., Guette, A., Naslein, R., Bourrat, X., 2005. Multiscale structure of sheet nacre. Biomaterials 26, 6254–6262.

Sandford, F., 2003. Physical and chemical analysis of the siliceous skeletons in six sponges of two groups (Demospongiae and Hexactinellida). Microsc. Res. Tech. 62, 336–355.

Schmidt, W.J., 1924. Die Bausteine des Tierkörpers in Polarisiertem Lichte. Verlag F. Cohen, Bonn.

Schulze, F.E., 1904. Hexactinellida. Wissenschaftliche Ergebnisse der deutschen Tiefsee-Expedition auf dem Dampfer "Valdivia" 1898–1899, vol. 4, Fischer, Jena.

Schwab, D.W., Shore, R.E., 1971. Fine structure and composition of a siliceous spicule. Biol. Bull. 140, 125–136.

Sethmann, I., Grassmann, O., Löbmann, P., Putnis, A., 2005. Observation of nano-clustered calcite growth via a transient phase mediated by organic polyanions: a close match for biomineralization. Am. Mineral. 90, 1213–1217.

Sethmann, I., Hinrichs, R., Putnis, A. Biomineral single-crystals: composite nano-cluster structures and polyanion-mediated growth model. In: Arias, J.L., Fernandez, M.S. (Eds.), Biomineralization: From Paleontology to Materials Science, Editorial Universitaria, Santiago de Chile, in press.

Sethmann, I., Hinrichs, R., Wörheide, G., Putnis, A., 2006. Nano-cluster composite structure of calcitic sponge spicules—a case study of basic characteristics of biominerals. J. Inorg. Biochem. 100, 88–96.

Simpson, T.L., 1984. The Cell Biology of Sponges. Springer-Verlag, New York.

Smith, A.B., 1990. Biomineralization in echinoderms. In: Carter, J.G. (Ed.), Skeletal Biomineralization: Patterns, Processes and Evolutionary Trends, vol. 1. Van Nostrand Reinhold, New York, pp. 413–443.

Sollas, W.J., 1885a. On the physical characters of calcareous and siliceous sponge-spicules and other structures. Sci. Proc. R. Dublin Soc. (N.S.) 4, 374–392.

Sollas, W.J., 1885b. Note on the artificial deposition of crystals of calcite on the spicules of a calci-sponge. Sci. Proc. R. Dublin Soc. (N.S.) 5, 73.

Stolarski, J., Mazur, M., 2005. Nanostructure of biogenic versus abiogenic calcium carbonate crystals. Acta Palaeontol. Polonica 50, 847–865.

Towe, K.M., 1967. Echinoderm calcite: single crystal or polycrystalline aggregate. Science 157, 1048–1050.

Travis, D.F., 1970. The comparative ultrastructure and organization of five calcified tissues. In: Schraer, H. (Ed.), Biological Calcification: Cellular and Molecular Aspects. Appleton-Century-Crofts, New York, pp. 203–311.

Travis, D.F., François, C.J., Bonar, L.C., Glimcher, M.J., 1967. Comparative studies of the organic matrices of invertebrate mineralized tissues. J. Ultrastruct. Res. 18, 519–555.

Tsipursky, S.J., Buseck, P.R., 1993. Structure of magnesian calcite from sea urchins. Am. Mineral. 78, 775–781.

Uriz, M.J., 2006. Mineral skeletogenesis in sponges. Can. J. Zool. 84, 322–356.

Uriz, M.J., Maldonado, M., 1995. A reconsideration of the relationship between polyaxonid and monaxonid spicules in Demospongiae: new data from the genera *Crambe* and *Discorhabdella* (Porifera). Biol. J. Linnean Soc. 55, 1–15.

Uriz, M.J., Turon, X., Becerro, M.A., 2000. Silica deposition in Demosponges: spiculogenesis in *Crambe crambe*. Cell Tiss. Res. 301, 299–309.

Uriz, M.J., Turon, X., Becerro, M.A., 2003a. Silica deposition in demosponges: spiculogenesis in *Crambe crambe*. Cell Tissue Res. 301, 299–309.

Uriz, M.J., Turon, X., Becerro, M.A., 2003b. Siliceous spicules and skeleton frameworks in sponges: origin, diversity, ultrastructural patterns, and biological functions. Microsc. Res. Tech. 62, 279–299.

Vacelet, J., Borojevic, R., Boury-Esnault, N., Manuel, M., 2002a. Order Lithonida Vacelet, 1981, recent. In: Hooper, J.N.A., Van Soest, R.W.M. (Eds.), Systema Porifera. Guide to the Supraspecific Classification of Sponges and Spongiomorphs (Porifera), vol. 2. Plenum, New York, pp. 1185–1192.

Vacelet, J., Borojevic, R., Boury-Esnault, N., Manuel, M., 2002b. Order Murrayonida Vacelet, 1981. In: Hooper, J.N.A., Van Soest, R.W.M. (Eds.), Systema Porifera. Guide to the Supraspecific Classification of Sponges and Spongiomorphs (Porifera), vol. 2. Plenum, New York, pp. 1153–1156.

von Ebner, V., 1887. Über den feineren Bau der Skelettheile der Kalkschwämme nebst Bemerkungen über Kalkskelete überhaupt. Sitzungsberichte der Kaiserlichen Akademie der Wissenschaften, 1. Abtheilung 95, 55–149.

Wainwright, S., Biggs, W.S., Currey, J.D., Gosline, J., 1975. Mechanical Design in Organisms. Edward Arnold, London.

Weaver, J.C., Morse, D.E., 2003. Molecular biology of demosponge axial filaments and their roles in biosilicification. Microsc. Res. Tech. 62, 356–367.

Weaver, J.C., Pietrasanta, L.I., Hedin, N., Chamelka, B.F., Hansma, P.K., Morse, D.E., 2003. Nanostructural features of demosponge biosilica. J. Struct. Biol. 144, 271–281.

Weber, J.N., 1969. The incorporation of magnesium into the skeletal calcites of echinoderms. Am. J. Sci. 267, 537–566.

Weber, J.N., 1973. Temperature dependence of magnesium in echinoid and asteroid skeletal calcite: a reinterpretation of its significance. J. Geol. 81, 543–556.

Weiner, S., Addadi, L., 1997. Design strategies in mineralized biological materials. J. Mater. Chem. 7, 689–702.

Weiner, S., Addadi, L., Wagner, H.D., 2000. Materials design in biology. Mater. Sci. Eng. C 11, 1–8.

Weinschenk, E., 1905. Ueber die Skeletteile der Kalkschwämme. Centralbl. Mineral. Geol. Paläontol. 19, 581–588.

Weiss, I.M., Gohring, W., Fritz, M., Mann, K., 2001. Perlustrin, a *Haliotis laevigata* (abalone) nacre protein, is homologous to the insulin-like growth factor binding protein N-terminal module of vertebrates. Biochem. Biophys. Res. Commun. 285, 244–249.

Woesz, A., Weaver, J.C., Kazanci, M., Dauphin, Y., Aizenberg, J., Morse, D.E., Fratzl, P., 2006. Micromechanical properties of biological silica in skeletons of deep-sea sponges. J. Mater. Res. 21, 2068–2078.

Woodland, W., 1905. Studies in spicule formation. I. The development and structure of spicules in Sycons: with remarks on the conformation, modes of disposition and evolution of spicules in calcareous sponges generally. Q. J. Microsc. Sci. 49, 231–282.

Wörheide, G., 1998. The reef cave dwelling ultraconservative coralline demosponge *Astrosclera willeyana* Lister 1900 from the Indo-Pacific. Micromorphology, ultrastructure, biocalcification, isotope record, taxonomy, biogeography, phylogeny. Facies 38, 1–88.

Wörheide, G., Hooper, J.N.A., 1999. Calcarea from the Great Barrier Reef. 1: Cryptic Calcinea from Heron Island and Wistari Reef (Capricorn-Bunker Group). Memoirs of the Queensland Museum 43, 859–891.

Wörheide, G., Hooper, J.N.A., 2003. New species of Calcaronea (Porifera: Calcarea) from cryptic habitats of the southern Great Barrier Reef (Heron Island and Wistari Reef, Capricorn-Bunker Group, Australia). J. Nat. Hist. 37, 1–47.